T.R.

GEBZE TECHNICAL UNIVERSITY

GRADUATE SCHOOL

COMPARISON OF THE FATIGUE BEHAVIOUR OF Ti-6Al-4V MATERIAL PRODUCED WITH CASTING AND ADDITIVE MANUFACTURING (EB-PBF)

KEREM SELVİ

A THESIS OF MASTER OF SCIENCE

DEPARTMENT OF ENERGY TECHNOLOGIES

APPLIED PROPULSION SYSTEM DESIGN AND ENGINEERING FOR AEROSPACE TECHNOLOGIES PROGRAM

ADVISOR: ASSIST. PROF. DR. MAHMUT AKŞİT

JULY 2024

T.R.
GEBZE TECHNICAL UNIVERSITY
GRADUATE SCHOOL

COMPARISON OF THE FATIGUE BEHAVIOUR OF Ti-6Al-4V MATERIAL PRODUCED WITH CASTING AND ADDITIVE MANUFACTURING (EB-PBF)

KEREM SELVİ

A THESIS OF MASTER OF SCIENCE
DEPARTMENT OF ENERGY TECHNOLOGIES
APPLIED PROPULSION SYSTEM DESIGN AND ENGINEERING FOR AEROSPACE TECHNOLOGIES PROGRAM

ADVISOR: ASSIST. PROF. DR. MAHMUT AKŞİT

JULY 2024

T.C.
GEBZE TEKNİK ÜNİVERSİTESİ
LİSANSÜSTÜ EĞİTİM ENSTİTÜSÜ

DÖKÜM VE KATMANLI İMALAT (EB-PBF) İLE ÜRETİLEN Ti-6Al-4V MALZEMESİNİN YORULMA DAVRANIŞININ KARŞILAŞTIRILMASI

KEREM SELVİ

YÜKSEK LİSANS
ENERJİ TEKNOLOJİLERİ ANABİLİM DALI
HAVACILIK VE UZAY TEKNOLOJİLERİNDE UYGULAMALI İTKİ SİSTEMİ TASARIM MÜHENDİSLİĞİ PROGRAMI

DANIŞMAN: DR. ÖĞR. ÜYESİ MAHMUT AKŞİT

TEMMUZ 2024

MASTER of SCIENCE JURY APPROVAL FORM

A thesis submitted by Kerem SELVİ, defended on 10/07/2024 before the jury formed with the 08/07/2024 date and 2024/35 numbered decision of the GTU Graduate Administration Board, has been accepted as a MASTER of SCIENCE thesis in the Department of Energy Technologies, Applied Propulsion System Design and Engineering Program for Aerospace Technologies.

JURY

MEMBER
(THESIS ADVISOR) : Assist. Prof. Dr. Mahmut AKŞİT

MEMBER : Assist. Prof. Dr. Recep ÖNLER

MEMBER : Assist. Prof. Dr. Mehmet Ekrem ÇAKMAK

APPROVAL

Gebze Technical University Graduate Administration Board

…..…/…..…/..…… date and ……/…….. numbered decision.

SIGNATURE/SEAL

ABSTRACT

Titanium alloy (Ti-6Al-4V) is widely used in the aerospace, automotive, and medical industries due to its high strength-to-weight ratio and biocompatibility. Both investment casting and additive manufacturing processes can be used to produce Ti-6Al-4V components, but it is important to investigate the differences in the fatigue behavior of these materials.

Fatigue is a critical concern in aerospace engineering, as components are subjected to cyclic loading conditions during operation, which can lead to material degradation and failure over time. Therefore, understanding the fatigue performance of materials is essential for ensuring the safety and reliability of aerospace structures and components.

The fatigue tests involve subjecting the specimens to cyclic loading at various stress levels and frequencies to simulate real-world operating conditions. The fatigue test data, including fatigue life, fatigue strength, stress-life curves, and other relevant parameters, are recorded and analyzed to assess the fatigue behavior of the specimens produced by each method.

The study aims to address the following objectives: first, to characterize the fatigue behavior of Ti-6Al-4V alloy specimens manufactured by EB-PBF and investment casting methods; second, to compare the fatigue properties of components produced by these two manufacturing processes; and third, to evaluate the feasibility of EB-PBF, one of the additive manufacturing method as a potential replacement for traditional methods such as investment casting in aerospace applications based on fatigue performance.

The results of the fatigue tests are compared to determine whether there are significant differences in fatigue performance between EB-PBF produced and investment casting produced specimens.

The findings contribute to the body of knowledge on the fatigue behavior of Ti-6Al-4V alloy components manufactured by different processes and provide valuable guidance for material selection and manufacturing process optimization in the aerospace industry.

Furthermore, the study sheds light on the potential of additive manufacturing technologies such as EB-PBF to revolutionize aerospace manufacturing by offering enhanced performance, reduced lead times, and increased design flexibility compared to traditional methods like investment casting.

Keywords: Additive Manufacturing (AM), Investment Casting, Electron Beam Powder Bed Fusion (EB-PBF), Fatigue Behaviour, Ti-6Al-4V Alloy.

ÖZET

Titanyum alaşımı (Ti-6Al-4V), yüksek mukavemet-ağırlık oranı ve biyouyumluluğu nedeniyle havacılık, otomotiv ve tıp endüstrilerinde yaygın olarak kullanılmaktadır. Ti-6Al-4V bileşenleri üretmek için hem hassas döküm hem de eklemeli üretim süreçleri kullanılabilir, ancak bu malzemelerin yorulma davranışlarındaki farklılıkları araştırmak önemlidir.

Yorulma, havacılık ve uzay mühendisliğinde kritik bir konudur, çünkü bileşenler çalışma sırasında döngüsel yükleme koşullarına maruz kalır ve bu da zaman içinde malzemenin bozulmasına ve arızalanmasına neden olabilir. Bu nedenle, malzemelerin yorulma performansını anlamak, havacılık yapılarının ve bileşenlerinin güvenliğini ve güvenilirliğini sağlamak için çok önemlidir.

Yorulma testleri, gerçek dünyadaki çalışma koşullarını simüle etmek için numunelerin çeşitli stres seviyelerinde ve frekanslarda döngüsel yüklemeye tabi tutulmasını içerir. Yorulma ömrü, yorulma mukavemeti, gerilme-yaşam eğrileri ve diğer ilgili parametreler dahil olmak üzere yorulma testi verileri, her bir yöntemle üretilen numunelerin yorulma davranışını değerlendirmek için kaydedilir ve analiz edilir.

Bu çalışma aşağıdaki hedefleri ele almayı amaçlamaktadır: birincisi, EB-PBF ve hassas döküm yöntemleriyle üretilen Ti-6Al-4V alaşım numunelerinin yorulma davranışını karakterize etmek; ikincisi, bu iki üretim süreci ile üretilen bileşenlerin yorulma özelliklerini karşılaştırmak; ve üçüncüsü, havacılık ve uzay uygulamalarında hassas döküm gibi geleneksel yöntemlerin yerine potansiyel bir alternatif olarak eklemeli üretim yöntemlerinden biri olan EB-PBF'nin fizibilitesini yorulma performansına göre değerlendirmeyi amaçlamaktadır.

Yorulma testlerinin sonuçları, EB-PBF ile üretilen ve hassas döküm ile üretilen numuneler arasında yorulma performansında önemli farklılıklar olup olmadığını belirlemek için karşılaştırılmıştır.

Bulgular, farklı proseslerle üretilen Ti-6Al-4V alaşım bileşenlerinin yorulma davranışı hakkındaki bilgi birikimine katkıda bulunmakta ve havacılık endüstrisinde malzeme seçimi ve üretim süreci optimizasyonu için değerli bir rehberlik sağlamaktadır.

Çalışma ayrıca, EB-PBF gibi eklemeli üretim teknolojilerinin, hassas döküm gibi geleneksel yöntemlere kıyasla daha yüksek performans, daha kısa teslim süreleri ve daha fazla tasarım esnekliği sunarak havacılık ve uzay üretiminde devrim yaratma potansiyeline ışık tutmaktadır.

Anahtar Kelimeler: Ti-6Al-4V Alaşımı, Yorulma Davranışı, Hassas Döküm, Toz Yatağında Elektron Işını Ergitme (EB-PBF), Eklemeli Üretim (EÜ).

ACKNOWLEDGEMENTS

I would like to express my deepest gratitude to my supervisor, Dr. Mahmut AKŞİT, for their unwavering support, guidance, and expertise throughout the process of researching and writing this thesis. Their insightful feedback, patience, and encouragement have been invaluable in shaping the direction and quality of this work.
I am also equally grateful to my co-supervisor, Dr. Ceylan KUBİLAY ERDEM, for their valuable contributions, feedback, and support. Their expertise and perspective have greatly enriched this thesis and enhanced its overall depth and rigor.
To my beloved spouse, Özlem SELVİ, your unwavering support, understanding, and encouragement have sustained me through the challenges of graduate study. Your love and patience have been my source of strength and motivation, and I am profoundly grateful for your presence in my life.
I am equally thankful to my dear child, Arya SELVİ, for bringing joy, laughter, and inspiration into my life every day. Your presence has been a constant reminder of what truly matters, and your enthusiasm has infused this journey with renewed energy and purpose.
I extend my heartfelt appreciation to all my colleagues, Emre DALAK, Taha Berkcan KILINÇ, Berktuğ ÜÇEL, Bahadır TAKIM who have supported and encouraged me along this academic journey.
Finally, I would like to express my gratitude to "TEI - Tusaş Engine Industries Inc." for providing the resources and environment necessary for me to pursue my academic aspirations. The opportunities and support offered by the institution have been instrumental in the completion of this thesis.

TABLE OF CONTENTS

LIST OF SYMBOLS AND ABBREVIATIONS

α	:	Alpha
β	:	Beta
Al	:	Aluminum
Ar	:	Argon
C	:	Carbon
CP Ti	:	Commercially Pure Titanium
Fe	:	Iron
H	:	Hydrogen
Mo	:	Molybdenum
MPa	:	Megapascal
N	:	Nitrogen
Nb	:	Niobium
Ni	:	Nickel
O	:	Oxygen
Si	:	Silicon
Sn	:	Tin
Ti	:	Titanium
TiAl	:	Titanium Aluminide
V	:	Vanadium
vol.	:	Volume
wt.	:	Weight
XY	:	Horizontal
Y	:	Yttrium
Z	:	Vertical
Zr	:	Zirconium
3D	:	Three Dimensional
AM	:	Additive Manufacturing
bcc	:	Body Centered Cubic
CAD	:	Computer Aided Design
CNC	:	Computer Numerical Control
DED	:	Directed Energy Deposition
EB-PBF	:	Electron Beam Powder Bed Fusion
EÜ	:	Eklemeli Üretim
HCF	:	High Cycle Fatigue
hcp	:	Hexagonal Close Packed
HIP	:	Hot Isostatic Pressing
IC	:	Investment Casting
LCF	:	Low Cycle Fatigue
L-PBF	:	Laser Powder Bed Fusion
PBF	:	Powder Bed Fusion
RP	:	Rapid Prototyping
STL	:	Stereolithography

LIST OF FIGURES

LIST OF TABLES

1. INTRODUCTION

Titanium and its alloys are well known for their versatility, finding applications across various sectors such as automotive, petrochemical, aerospace, and biomedical. Their exceptional attributes, including a high strength-to-weight ratio and remarkable corrosion resistance, make them a top choice. Particularly, Ti-6Al-4V, constituting over 25% of aero engine disks and blades in the fan and compression sections operating at approximately 500°C, offers superior specific strength at elevated temperatures compared to aluminum alloys while being lighter than steel and nickel alloys. Furthermore, Ti-6Al-4V is biocompatible and corrosion-resistant, making it suitable for medical implants **[1]**.

Heat treatment, fabrication methods, mechanical working of ingots, the melting process to form the ingot, and the types and amounts of alloyants and impurities within the ingot all have a significant impact on the titanium product's physical and mechanical properties. The processing environment and conditions surrounding titanium and its alloys must be carefully controlled. While a narrow range of titanium alloys serves many different kinds of uses, altering the conditions of mechanical or thermal processing allows for producing a greater variety of titanium and its alloys **[1]**, **[2]**.

The Ti-6Al-4V alloy exists in cast, wrought, and additive manufacturing (AM) forms and finds widespread use in the aerospace industry. The strain rate of deformation and temperature significantly influences the alloy's final microstructure and subsequent mechanical properties. During elevated temperatures, the deformation in the alloy plays a crucial role in determining its mechanical characteristics. Ti-6Al-4V is recognized for its excellent plastic deformability compared to aluminum and steel alloys **[2], [3]**.

In investment casting (IC), a wax pattern is created using an injection molding technique or prototyping with AM. The wax or wax injection tooling cavity is purposely oversized, considering the wax, ceramic shell and titanium alloy shrinkages. The wax pattern is supplemented with a gating system pattern. Subsequently, the pattern assembly undergoes multiple cycles of dipping in ceramic slurries, stuccoing

and drying to build a robust ceramic shell capable of withstanding molten metal pressure upon firing. The wax pattern is taken out in a steam autoclave, creating a mold cavity that is prepared for casting following firing. The casting can be done by gravity pouring, which requires preheating the shells to a higher temperature in order to enhance the flow of molten metal, or by using a centrifugal table to aid in the metal's flow. After casting and solidification, post-casting operations are conducted. These can be listed as 1) knocking-out to remove ceramic mold from casting, 2) cutting off the metal mold to separate gating and casting part if needed, 3) core removal to distract core from casting, 4) heat treatment to provide mechanical requirements and stress relief, 5) abrasive cleaning to leave casting in clean condition, etc. Hot isostatic pressing (HIP), another post-casting procedure, is being used frequently for steel, aluminum, and superalloys and is becoming more popular as a way to improve characteristics and remove porosity, particularly for titanium **[4]**.

Based on the feeding of raw materials, AM methods can be divided into two major groups: directed energy deposition (DED) and powder bed fusion (PBF). Within PBF, which includes electron beam and laser beam methods, several approaches are used to produce Ti-alloy components. Laser-produced parts offer superior surface finish but may suffer from issues like high residual stress and the formation of martensitic microstructures due to rapid cooling. On the other hand, with their higher energy input and slower cooling, electron beam techniques enable the creation of intricate geometries with over 99% relative density and reduced residual stresses. However, parts with rough surfaces may require post-processing to enhance their mechanical properties **[5]**.

Currently, electron beam powder bed fusion (EB-PBF) is widely used for producing intricate Ti-6Al-4V alloy components. In EB-PBF, components are constructed layer by layer using micron-sized Ti-6Al-4V alloy powders deposited onto the build platform and subsequently melted by a high-vacuum electron beam. Pre-heating in production helps reduce residual stresses and avoids martensitic phase formation by carefully controlling the cooling process above the martensitic start temperature. Consequently, Ti-6Al-4V parts produced through EB-PBF exhibit microstructures characterized by α-phase plates with limited β-phase content arranged in a Widmanstätten structure that grows throughout the fabrication orientation. Furthermore, optimizing key process parameters, including focus offset, line energy,

layer thickness, and electron beam current, can provide parts with enhanced density **[5], [6]**.

While EB-PBF offers numerous advantages, it does come with some drawbacks. These drawbacks include increased surface roughness due to internal stresses resulting from temperature gradients, partially melted powders, and imperfections such as porosity, delamination, lack of fusion, and balling post-production. Additionally, it leads to anisotropic mechanical properties based on the build direction and varying density across the production plate **[5]**.

Various post-processing methods are employed for EB-PBF samples. For instance, methods like milling, chemical polishing, blasting, and machining can be applied to improve surface roughness. Heat treatments like HIP and traditional annealing are employed to decrease residual stress. HIP aims to reduce porosity and achieve parts with 100% relative density, though traditional annealing may reduce alloy strength while increasing ductility. Although heat treatment cannot refine the grain structure, it can lead to finer microstructures **[7]**.

AM for Ti-6Al-4V alloys provides several advantages over conventional production methods. It enables the consolidation of an assembly into a single part. Traditional manufacturing of complex parts often involves multiple steps, increased material consumption, higher labor costs, and extended assembly time, leading to larger inventory requirements. AM offers a more efficient approach. It is possible to produce the entire assembly as a single, integrated piece by employing additive manufacturing. This approach saves money and reduces production time from start to finish. Additive manufacturing significantly streamlines the rapid prototyping process, making it more manageable within strict deadlines and budget constraints.

In contrast, the costs associated with computer numerical control (CNC) milling setups, investment casting, and their subtractive processes can be substantial. With AM, prototype expenses are comparatively more affordable, making it a cost-effective choice for iterative testing and design adjustments. The iterative nature of AM facilitates smooth design modifications. Engineers can easily adjust the design, produce the new part, and promptly evaluate whether the updated design meets the desired requirements. This near-instant feedback allows efficient and cost-effective design optimization during prototyping **[5]-[7]**.

Fatigue is a critical issue in aerospace engineering, as in many industries, because systems are exposed to cyclic loadings during operation, which can cause material failure and breakdown over time. Therefore, understanding the fatigue performance of materials is necessary to maintaining the safety and reliability of aerospace structures and components **[2], [3]**.

This thesis comprises five main chapters, providing insights into the fatigue characteristics of Ti-6Al-4V material manufactured using investment casting and EB-PBF. Chapter 2 presents the literature review, covering topics such as titanium properties, investment casting, and AM technology, focusing on Ti-6Al-4V, including its mechanical, chemical, and microstructural characteristics. In Chapter 3, we provide detailed information about the experimental arrangement, including the physical and chemical characteristics of the specimens. This chapter also introduces various characterization methods, including compositional analysis, mechanical testing, and fatigue measurements. Chapter 4 encompasses the experimental results and their discussions concerning fatigue characteristics. Consequently, Chapter 5 offers conclusions along with prospective future works.

2. LITERATURE REVIEW

2.1. Titanium and Titanium Alloys

Titanium (Ti) and its alloys are widely used in diverse engineering fields because of their remarkable properties, which include high melting point, low density, favorable mechanical properties, and good corrosion resistance **[1]**.

Titanium is categorized as a non-ferrous metal and is recognized as the heaviest among lightweight metals, with a density of 4.51 g/cm^3, as represented in **Figure 2.1**. Notably, titanium possesses a high specific strength, particularly at elevated temperatures, as illustrated in **Figure 2.2**. Consequently, Titanium Aluminide (TiAl) based alloys are in a direct competitive relationship with Nickel (Ni) based superalloys and high-temperature steels, as seen in **Figure 2.2 [2]**.

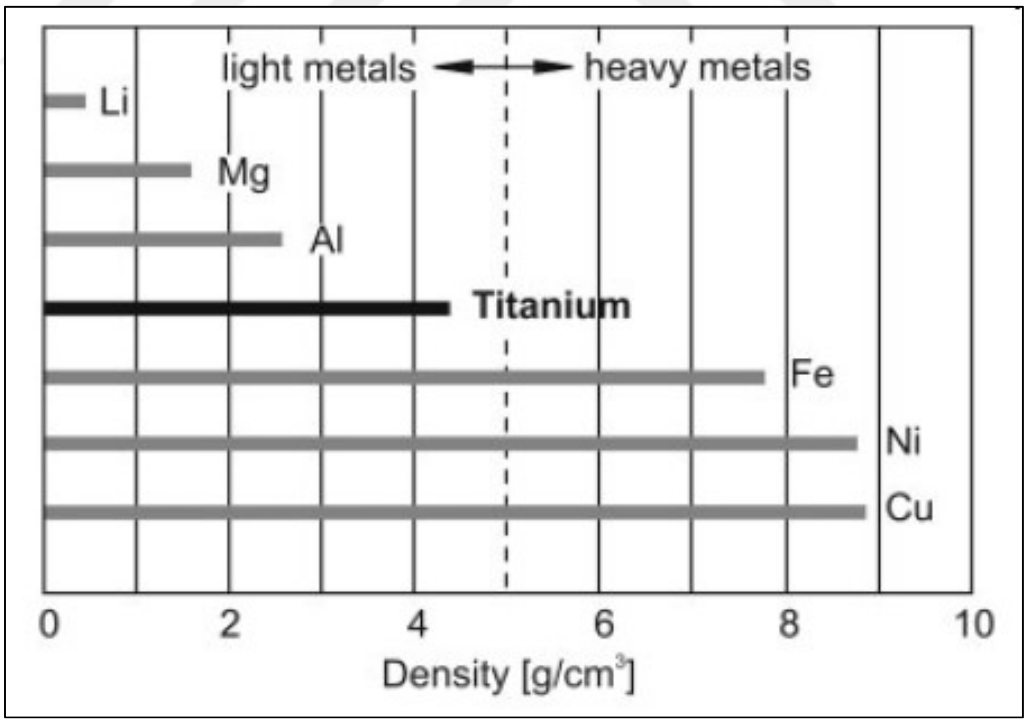

Figure 2.1 : Comparing the densities of light and heavy metals. Adapted from **[2]**.

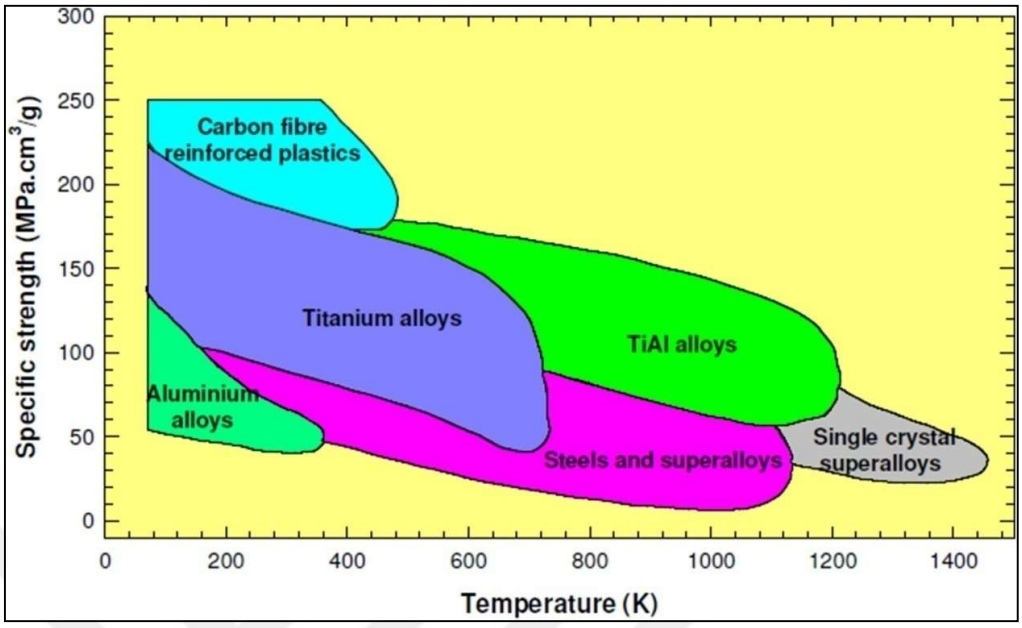

Figure 2.2 : Relationship between specific strength and temperature for chosen materials. Adapted from **[2]**.

These attributes enable the versatile use of Ti and its alloys in both structural and functional roles across multiple industries like aerospace, biomedical, automotive, and chemical **[1]**.

In aerospace, titanium alloys are chosen primarily for their lower density, allowing for weight reduction compared to steel. These alloys maintain higher strength than aluminum alloys, particularly at elevated temperatures, making them preferable for high-temperature applications over aluminum alloys. Furthermore, despite its higher density of approximately 60%, substituting titanium for aluminum still allows for weight savings **[8]**.

2.2. Properties and Metallurgy of Titanium

Titanium possesses non-magnetic properties and exhibits favorable heat-transfer characteristics. In comparison to steel, it has a lower coefficient of thermal expansion, and its coefficient is less than half that of aluminum. While steels have lower melting points than titanium and its alloys, depending on composition, the maximum temperatures at which titanium and its alloys can be used for structural purposes usually vary from 427 °C to roughly 538 °C to 595 °C. Titanium aluminide alloys in

particular exhibit potential for use in applications at temperatures as high as 760 °C **[1]**.

While titanium has a relatively high specific strength compared to other metals, its cost increases due to the expensive production method known as the Kroll process. This increased cost is mainly attributed to titanium's strong reactivity with oxygen. Consequently, the production process necessitates using a vacuum or inert atmosphere to prevent oxygen contamination. Conversely, titanium readily forms a thin surface oxide layer upon exposure to air, owing to its high affinity for oxygen. This thin oxide layer offers excellent corrosion resistance, which makes it a favored option for diverse fields **[9]**.

Pure titanium and most titanium alloys crystallize at low temperatures in a modified hexagonal close-packed (hcp) structure known as alpha (α) titanium. At high temperatures, however, the stable structure shifts to a body-centered cubic (bcc) configuration called beta (β) titanium. For pure titanium, the β-transus temperature is approximately 882 °C. The atomic unit cells of the body-centered cubic (bcc) β titanium and the hexagonal close-packed (hcp) α titanium are shown schematically in **Figure 2.3**, emphasizing their most tightly packed planes and orientations **[2]**.

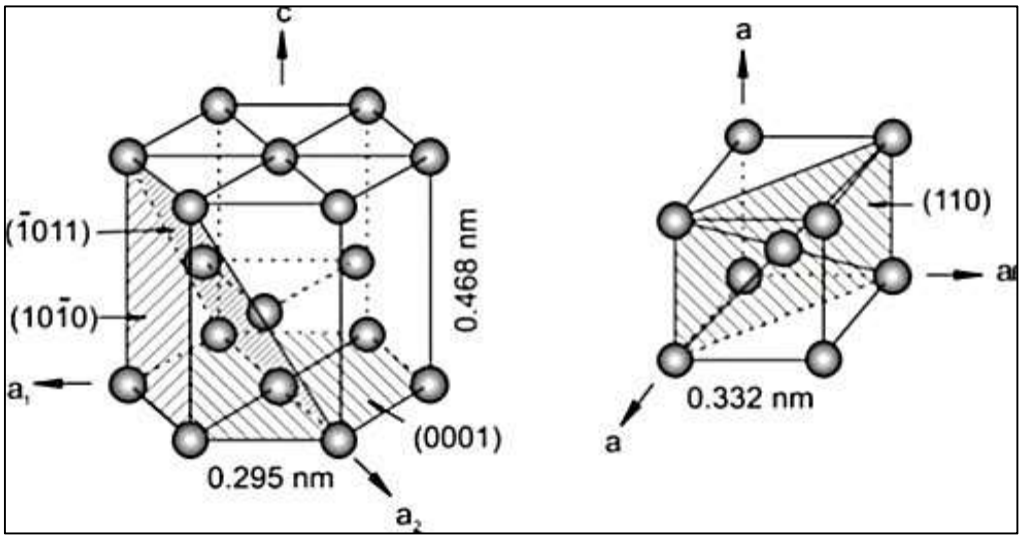

Figure 2.3 : The unit cells of the hcp α and bcc β titanium. Adapted from **[2]**.

Based on their effect on the β-transus temperature, the alloying elements in titanium are categorized as neutral, α-stabilizers, or β-stabilizers as shown in **Figure 2.4**. α-stabilizing elements expand the temperature range of the α phase while β-stabilizing

elements shift the temperature range of the β phase. Neutral elements have minimal influence on the β-transus temperature **[2]**.

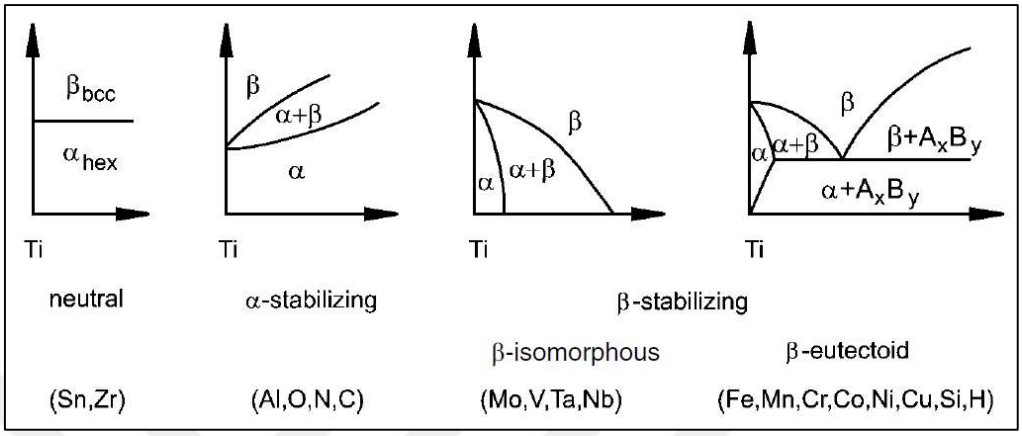

Figure 2.4 : The effect of alloying elements on phase diagrams in Titanium. Adapted from **[2]**.

2.3. Titanium Alloy Classifications

Different kinds of titanium alloys exist, distinguished by their composition and the predominant constituent phases at room temperature, each serving a specific purpose. It is customary to classify titanium alloys into four distinct categories based on the typical phases present. These alloy categories are commonly referred to as alpha (α) alloys, near (α) alloys, alpha (α) + beta (β) alloys and beta (β) alloys **[1], [10]**. The type and content of the alloys impact the properties, as shown in **Figure 2.5 [1]**.

2.3.1. Alpha Alloys

Alpha-phase alloys include commercially pure titanium (CP Ti), consisting mainly of the hexagonal close-packed (HCP) α-phase, with small (<5 vol. %) amounts of the β phase due to the existence of iron (Fe). The presence of Fe in CP Ti can be attributed to either residual impurities originating from the raw material, known as sponge, or intentional additions made during the manufacturing process. Based on composition, CP Ti is divided into four categories, with corresponding tensile strengths between 240 and 550 MPa for each grade **[11]**.

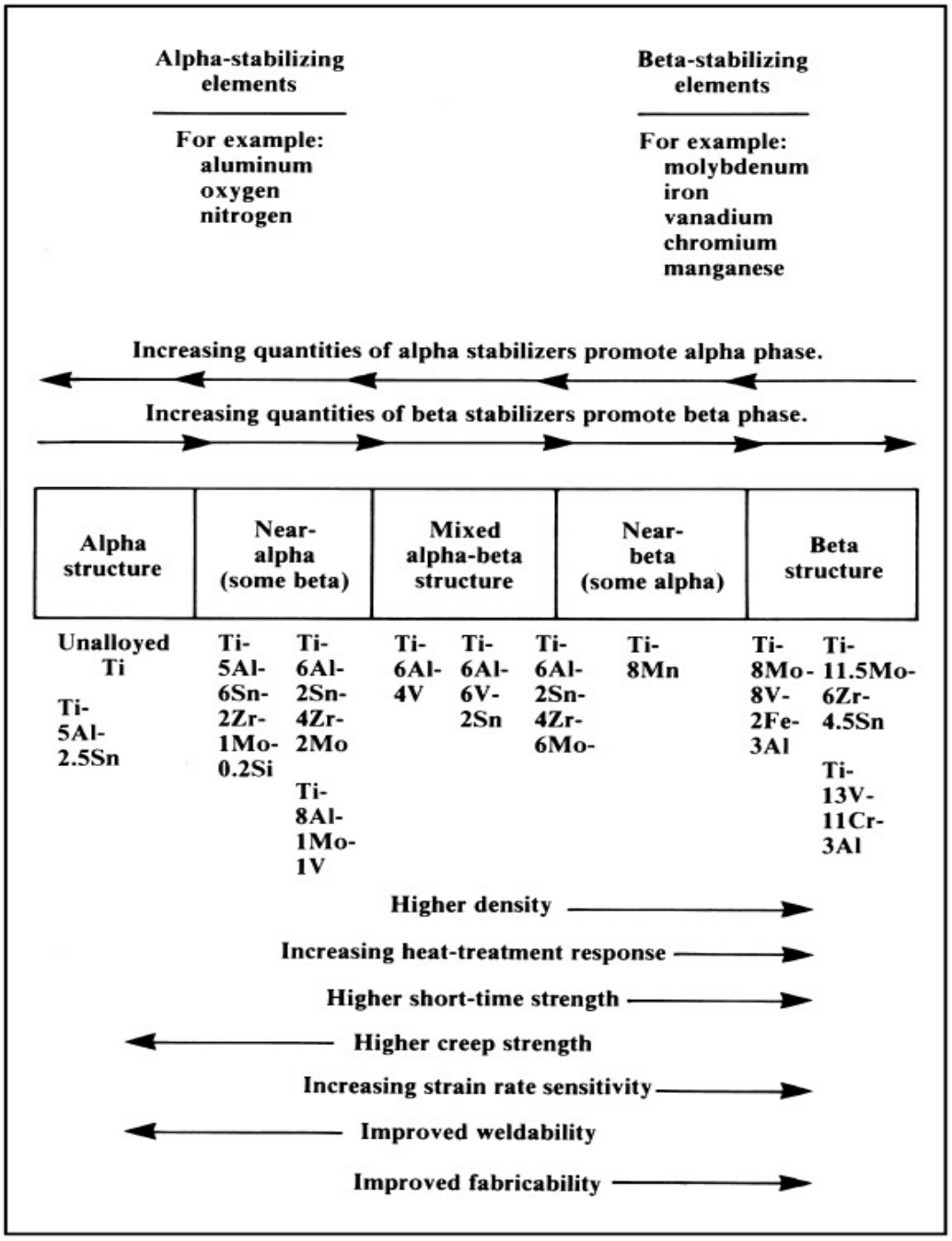

Figure 2.5 : Influence on specific alloy properties and content. Adapted from **[1]**.

The higher numbered grades demonstrate greater strength, primarily due to escalating oxygen concentrations. Oxygen is an essential element within CP Ti, serving as a potent solid solution strengthener. CP Ti finds its primary utility in applications where corrosion resistance and weldability are essential, without necessitating the higher strength properties characteristic of other titanium alloy classes **[9]**.

2.3.2. Near Alpha Alloys

They are mainly composed of aluminum (Al), tin (Sn), and zirconium (Zr) with minor additions (up to about 2 wt. %) of low diffusivity beta-stabilizers like molybdenum (Mo) or niobium (Nb) along with a limited amount of silicon (Si) limited to 0.5 wt. %. Mo and Nb stabilize small portions of the beta-phase at room temperature, increasing alloy strength and aiding controlled microstructure development during processing, resulting in enhanced properties and ease of fabrication. As these alloys are utilized in high temperature situations where creep strength is more important than tensile qualities, heat treatment is typically insufficient in modifying the strength of these alloys. Ti-6-2-4-2S, which can withstand temperatures up to around 540°C depending on the load, and IMI 834, which is appropriate for temperatures up to about 600°C, are two frequently used near alpha alloys. The highest temperature-capable, near-alpha titanium alloy currently being produced commercially is IMI 834. These near-alpha alloys have outstanding creep resistance and a good mix of other qualities, such as fatigue resistance, good weldability, tensile ductility, and damage tolerance, even though they cannot be heat treated for greater strength. **[9], [12]**.

2.3.3. Alpha + Beta Alloys

The α + β titanium alloys are widely used in structural applications and contain higher β stabilizer contents, usually in the range of 4% to 6% (wt.%), resulting in a greater β phase proportion compared to near alpha alloys. As these alloys contain beta stabilizers, heat treatment can be applied to them to increase their strengths. The principal process of strengthening is the change of metastable β phase into martensite upon quenching, or its retention at normal temperature. Aging conditions with metastable β phase lead to the formation of lamellar alpha regions, and these regions are enhancing the strength of material with minimal ductility reduction. Ti-6Al-4V (Ti-6-4) is the most widely utilized of these alloys due to its advantageous characteristics. Ti-6-4 has a minimum tensile strength of 896 MPa and is usually utilized in the annealed state. **[9], [12]**.

α + β alloys are generally weldable in inert environments, but for some high-strength alloys, precautions like pre-heating may be required **[9], [12]**.

Figure 2.6 illustrates the properties of α + β alloys. Ti-6Al-4V alloys find extensive use in various industrial sectors and academic research fields due to their unique blend of properties inherited from both α and β alloys. Examples of α + β alloys include Ti-6Al-4V, Ti-7Al-4Mo, Ti-3Al-2.5V and Ti-6Al-6V-2Sn. These alloys offer versatile material properties, making them appropriate for a variety of applications **[1], [2], [9], [11], [12]**.

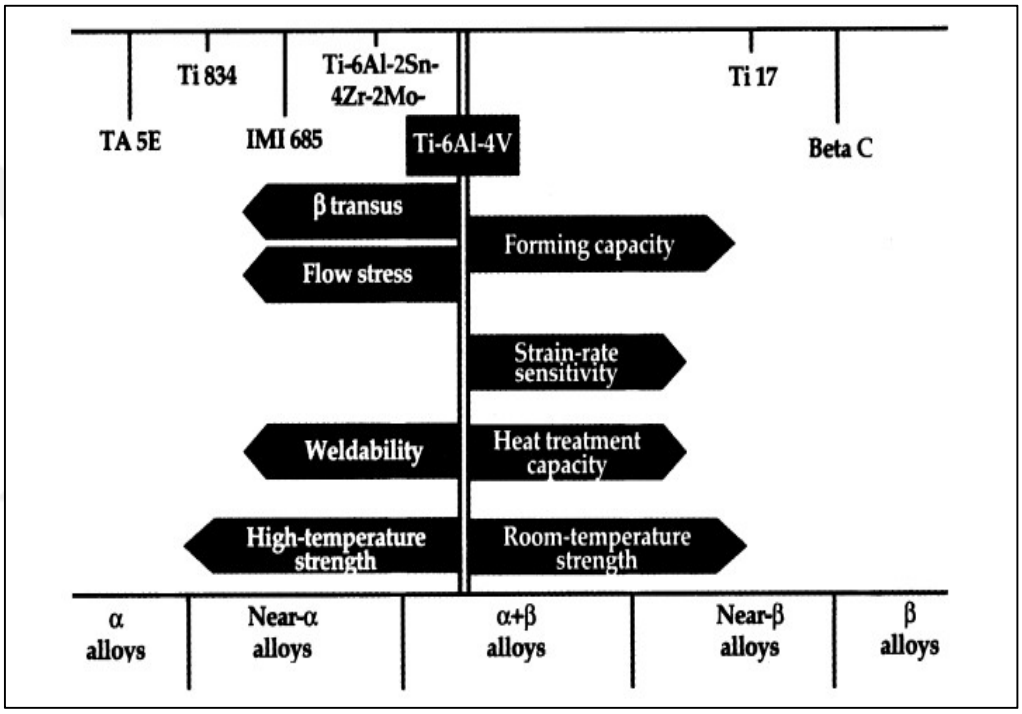

Figure 2.6 : Titanium alloys exhibit diverse characteristics and properties. Adapted from **[1]**.

2.3.4. Beta Alloys

Beta alloys containing transition elements including vanadium (V), niobium, and molybdenum are crucial for promoting the generation of the bcc β phase by lowering the temperature at which the α to β phase transition occurs. These alloys possess superior forgeability across a considerably higher forging temperature range compared to α alloys **[13], [14]**.

Beta alloys are known for their exceptional strength in the titanium alloy family. Once they quickly cool down from the β phase area, they maintain a completely metastable β phase at room temperature. As they age, α phase precipitation strengthens them.

Their greater strength compared to α + β alloys can be attributed to the controllable size and quantity of α phase precipitates within the β phase matrix by temperature and time adjustments during aging. Notable examples include Ti-6-2-4-6, Ti-17, Ti-10-2-3, Ti-5-5-5-3 and Ti-15-3-3-3. Ti-6-2-4-6 and Ti-17 are commonly utilized in modern, larger aircraft engines due to their increased strength **[1], [11], [12], [15]**.

2.4. Ti-6Al-4V Alloy

Ti-6Al-4V is an α + β alloy with 6 wt. % aluminum stabilizing the α phase and 4 wt. % V stabilizing the β phase. When cooled progressively from the elevated temperature β phase zone, it mostly comprises of around 90% hcp α phase and 10% metastable bcc β phase at room temperature. Different proportions of α and β phases and various microstructures, including grain boundary allotriomorph α, martensitic, primary or globular α, basketweave, and Widmanstätten structures, result from specific heat treatments and cooling rates during processing **[16]**.

The main mechanical characteristics and composition of AM, casting, and wrought Ti-6Al-4V alloys exhibit striking similarities, highlighting the material's inherent strength and versatility. Notable distinctions observed concerning ASTM standards, as detailed in **Table 2.1** and **Table 2.2**, emphasize the critical need to choose a manufacturing process that aligns with specific engineering demands. This analysis offers valuable insights for engineers and material scientists to make informed choices regarding the optimal utilization of Ti-6Al-4V alloys across diverse applications **[17]**.

Table 2.1 : The mechanical characteristics of Ti-6Al-4V alloys in AM, casting and wrought processes conforming to ASTM standards.

Standard	YS (MPa)	UTS (MPa)	Elongation %	Reduction of Area %
ASTM F1108-14	758	860	8	14
ASTM F136-13	795	860	10	25
ASTM F2924-14	825	895	10	15

Table 2.2 : The elemental composition of AM, cast and wrought Ti-6Al-4V alloys per ASTM standards.

Element	Chemical Composition (wt. %)		
	ASTM F1108-14 (cast)	**ASTM F136-13 (wrought)**	**ASTM F2924-14 (AM)**
Al	5.50 to 6.75	5.50 to 6.50	5.50 to 6.75
V	3.50 to 4.50	3.50 to 4.50	3.50 to 4.50
Fe	0.30 max.	0.25 max.	0.30 max.
O	0.20 max.	0.13 max.	0.20 max.
C	0.10 max.	0.08 max.	0.08 max.
N	0.05 max.	0.05 max.	0.05 max.
H	0.015 max.	0.015 max.	0.015 max.
Titanium	0.015 max.	Balance	Balance

The properties of α+β titanium alloys undergo notable variations in response to changes in microstructure. The microstructure in these alloys undergoes a complex series of thermomechanical processes, including solution heat treatment, stress relief annealing, aging, and recrystallization **[7]**.

The structural composition of the Ti-6Al-4V alloy significantly influences its mechanical properties. Cooling rates from the β phase region affect the size and layout of α and β phases, resulting in diverse microstructures: lamellar, equiaxed, bimodal, and martensitic. Lamellar structures, with higher α/β surface area, result from homogenization and stress-relieving heat treatment. Equiaxed structures featuring uniform α grains and β grain boundaries are achieved through recrystallization. While equiaxed structures show greater fatigue initiating resistance but inferior fatigue propagation resistance, lamellar structures offer superior fatigue propagation resistance, fracture toughness, and lower strength and tensile ductility. Solution heat treatment is used to create bimodal microstructures, which combine equiaxed primary α in a lamellar α+β matrix. Because of the benefits of both equiaxed and lamellar microstructures, they offer a balanced combination of fatigue characteristics, with higher resistance to fatigue fracture initiation and propagation. Martensitic

microstructures result from rapid quenching above the β transus temperature, yielding a hard and brittle alloy **[2], [15], [16]**.

Apart from the mentioned microstructures, the Ti-6Al-4V alloy also exhibits the Widmanstätten microstructure, sometimes also called the basketweave microstructure. This distinct microstructure resembles a specialized lamellar structure featuring parallel α phase plates intersected by the β phase. The Widmanstätten microstructure is a remarkable feature in the Ti-6Al-4V alloy, the formation of which is linked to rapid cooling from elevated temperatures. This unique structure, with its parallel α phase plates intersected by the β phase, requires precise cooling rates for its development. **Figure 2.7** illustrates the development of the Widmanstätten microstructure, demonstrating its formation during gradual cooling from the β region to the α region **[1], [7], [17]**.

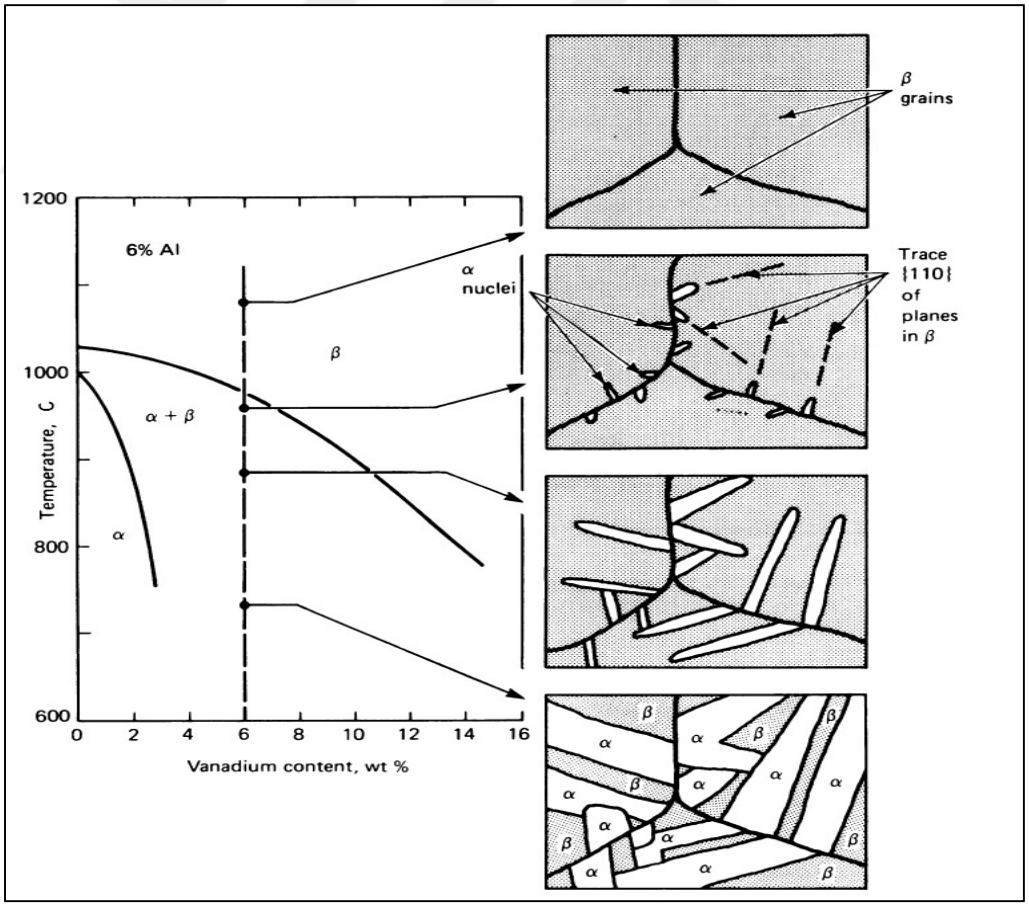

Figure 2.7 : Widmanstätten structure in an alpha-beta alloy (Ti-6Al-4V). Adapted from **[1]**.

Furthermore, the microstructural alterations in the Ti-6Al-4V alloy during annealing at different cooling rates and temperatures are compiled in **Figure 2.8**. These microstructural variations significantly influence the material's mechanical properties and are crucial in determining its performance under specific conditions **[1]**.

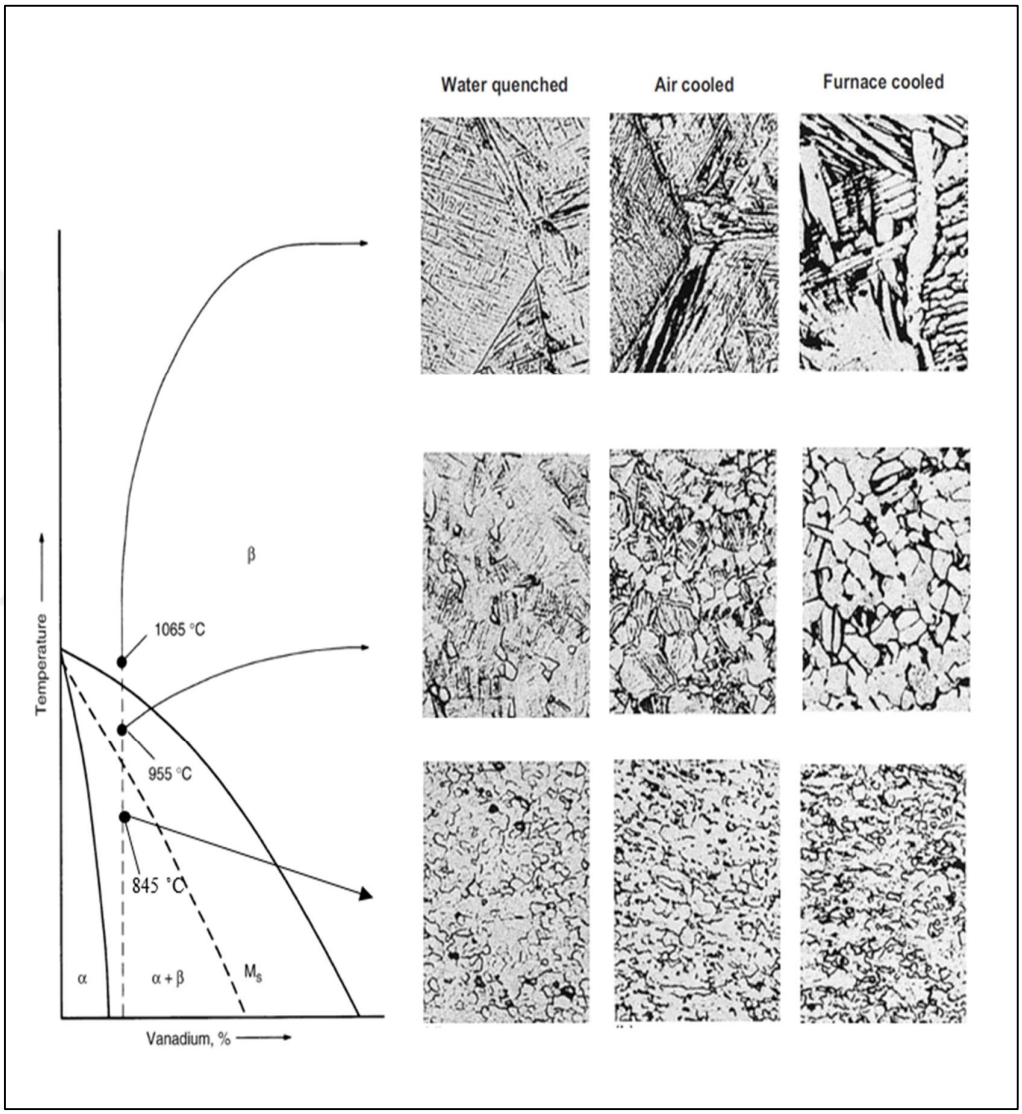

Figure 2.8 : Temperature and cooling rate's influence on Ti-6Al-4V alloy microstructure. Adapted from **[1]**.

The mechanical properties of α + β titanium alloys, namely the size and thickness of α lamellae colonies, are greatly influenced by the lamellar microstructure. Among these factors, the size of α colonies plays a substantial role in determining mechanical properties. It directly affects the thicknesses of α and β phases and slip lengths, resulting in variations in mechanical behavior **[7], [15]**.

Higher cooling rates reduce α colony size and slip length, leading to increased high cycle fatigue (HCF) strength and yield strength, indicating better crack resistance. Conversely, smaller slip length or colony size decelerates microcrack propagation, enhancing resistance to low cycle fatigue (LCF). Ductility exhibits a complex trend, increasing with reduced colony size due to less primary α phase formation at grain boundaries during rapid cooling but decreasing when a martensitic microstructure with smaller α colonies forms **[7], [15], [16]**.

2.5. Investment Casting

2.5.1. Basic Information About Investment Casting

Investment casting (IC), also often referred to as "precision casting" or "lost wax casting," stands as a time-tested and versatile manufacturing process known for its ability to create intricate metal components with remarkable precision. Investment cast parts encompass a diverse spectrum of metal alloys, including stainless steels, aluminum, low alloy steels, and nickel alloys. This method has proven indispensable in aerospace, automotive, jewelry, and beyond, where intricate geometries and exacting tolerances are essential **[18], [19]**.

2.5.2. Process Steps of Investment Casting

Investment casting constitutes a multi-stage manufacturing procedure meticulously employed for the fabrication of intricate and highly precise metal components. As shown in **Figure 2.9 [20]**, the process can be summarized in the following steps: Wax pattern making, wax assembly, slurry coating and stuccoing, dewaxing, pre-heating of the ceramic mold, casting, cooling and solidification, shell removal, cutting off the assembly, finishing, and inspection. Detailed information on the process steps has been given as follows **[19]**.

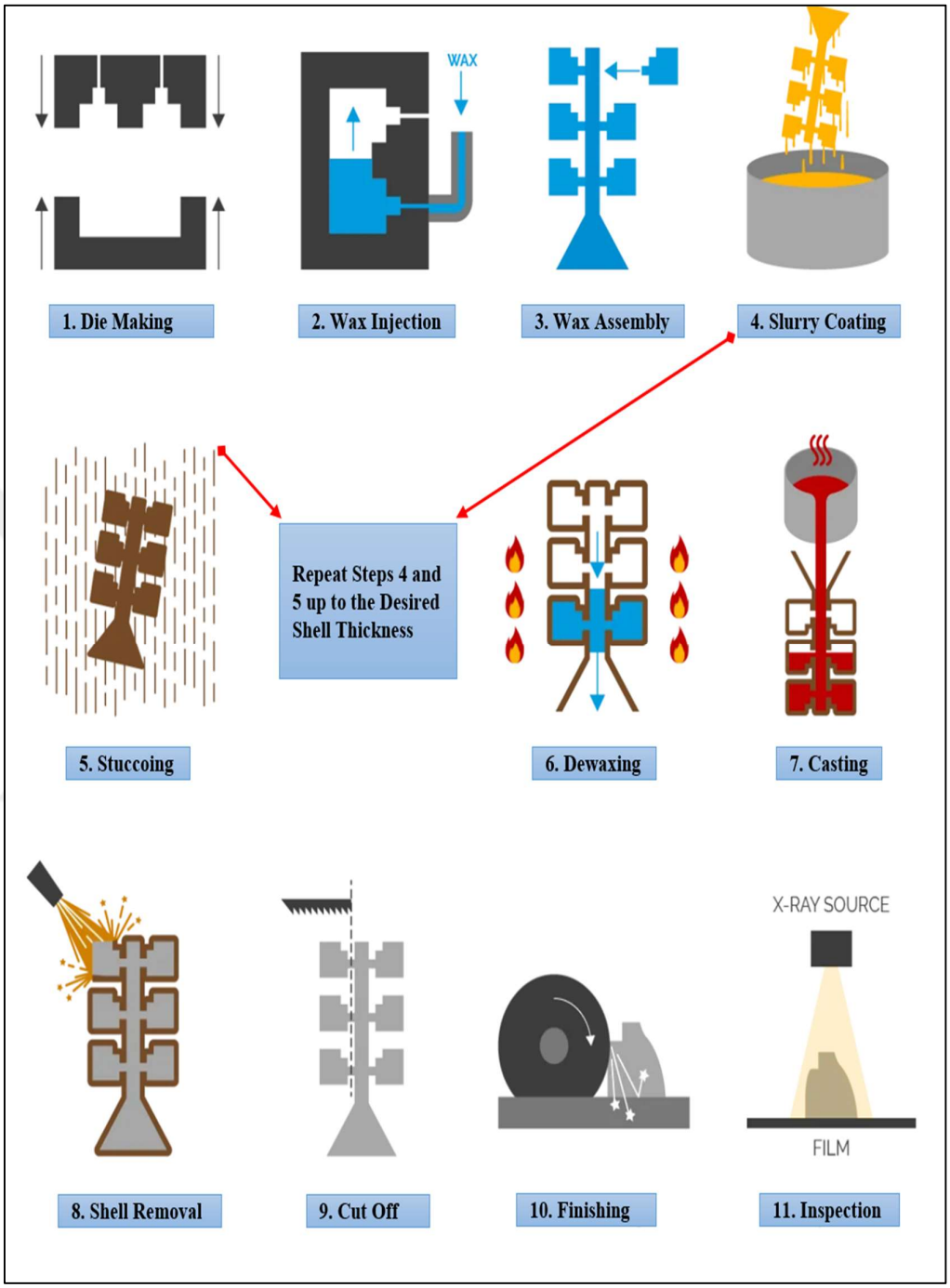

Figure 2.9 : Visual representation of sequential stages in investment casting. Adapted from **[20]**.

2.5.2.1. Wax Pattern Making

The investment casting process begins with the fabrication of pattern which is an exact replica of the requested part. Wax is used to make the pattern. These patterns are

produced through techniques like injection molding or three-dimensional (3D) printing. If a wax injection die is selected, the initial phase entails designing and constructing a precision metal die. This die is used to create a wax replica of the desired pattern through the injection of molten wax at elevated pressures into the designated cavity. Depending on volume needs, the die's complexity can range from a simple manual tool with one cavity to a complicated automated tool with multiple cavities. In the event that a 3D printed pattern is chosen, the process starts by sending a computer-aided design (CAD) model, which contains the exact geometry of the desired pattern, to a 3D printer. Subsequently, the desired pattern is fabricated through the 3D printing process **[4], [19], [21], [22]**.

2.5.2.2. Wax Assembly

Multiple patterns, representative of the desired quantity of parts, are strategically attached to a central gating system, forming a cluster or tree-like structure. This assembly optimizes the flow of molten metal into each individual pattern during the casting phase **[4], [19], [21], [22]**.

2.5.2.3. Slurry Coating and Stuccoing

One of the most critical stages of investment casting is the creation of the ceramic shell. The pattern assembly is immersed in a refractory slurry, often consisting of ceramic materials, and subsequently coated with a fine ceramic stucco. This layering process is repeated multiple times, allowing each application to dry between coats, resulting in a robust ceramic shell enveloping the entire pattern assembly **[4], [21]**.

2.5.2.4. Dewaxing

Following the solidification of the ceramic shell, the assembly undergoes a dewaxing process. This process entails heating the assembly in an autoclave or furnace to melt and eliminate the wax or plastic pattern, leaving behind an intricate, hollow ceramic mold. This step is fundamental to the "lost wax" nature of the casting process **[4], [19], [21], [22]**.

2.5.2.5. Pre-Heating of the Ceramic Mold

Before pouring the molten metal, the ceramic shell is pre-heated to a precise temperature. This pre-heating is critical to prevent thermal shock during casting and to ensure the proper flow of the molten metal **[4], [19], [21], [22]**.

2.5.2.6. Casting

Melted metal is carefully poured via the gating system into the hollow mold after the ceramic shell has been prepared and heated. The metal fills the void left by the removed pattern, taking on its exact shape. Typically, casting is conducted in a controlled atmosphere or under vacuum conditions to minimize the occurrence of defects **[19], [21], [22]**.

2.5.2.7. Cooling and Solidification

After pouring the molten metal, the entire assembly is allowed to cool and solidify within the ceramic shell. This stage is necessary to achieve the requested metallurgical properties and dimensional accuracy of the final component **[4], [21]**.

2.5.2.8. Shell Removal

Once the cast part has sufficiently cooled and solidified, the ceramic shell is carefully removed, revealing the cast metal part in its intricate detail **[4], [19], [21]**.

2.5.2.9. Cut-Off the Assembly

Following the removal of the shell, the parts are cut with liquid nitrogen or a vibrating saw to remove them from the runner and gating system **[4], [19], [21]**.

2.5.2.10. Finishing

The cast part might occasionally go through post-processing procedures like surface polishing, machining, and heat treatment. These finishing touches are performed to meet specific tolerances and quality standards, ensuring the final component meets its intended purpose **[4], [19], [21], [22]**.

2.5.2.11. Inspection

Before casting parts are shipped, the inspection step is one of the most important steps in investment casting production processes. Visual and fluorescent penetrant inspection methods are used to detect defects on the part surface, while X-ray inspection is used to detect indications inside the part **[4], [19], [21], [22]**.

2.5.3. Ti and Ti-6Al-4V Alloy Manufactured by Investment Casting

Titanium castings have been effectively integrated as economical substitutes for forged and wrought components in high-performance and progressively cost-sensitive sectors, including military and commercial aircraft airframe structures. Certain titanium castings have been manufactured at a fraction of the cost compared to similar forged and machined parts. Over the past two decades, investment casting has stood as the favored manufacturing approach for producing intricate titanium castings **[2]**.

Titanium alloy Ti-6Al-4V, with the same chemical composition as its wrought counterpart, possesses remarkable casting characteristics. Nonetheless, the elevated reactivity of titanium in its molten state necessitates the application of suitable casting technologies, which has subsequently constrained the number of foundries capable of working with titanium **[9]**.

It's pertinent to mention that Ti-6Al-4V castings are approximately two to three times more expensive than their superalloy counterparts. The cost-effectiveness of utilizing Ti-6Al-4V castings is contingent upon factors such as size, complexity, and the quantity of castings required **[9]**. Predominantly, these castings find significant application within the aerospace and marine industries. Furthermore, their utilization extends to various industrial sectors, including well-logging equipment for the petroleum industry, specialized automotive components, boat deck hardware, and medical implants **[23]**.

A Widmanstätten structure within a Ti-6Al-4V alloy is renowned for its exceptional specific strength, fracture toughness, and resistance to crack propagation, as referenced in **[16]**. This structure typically comprises colonies where thin α platelets align within a β matrix. A prime illustration of the Widmanstätten structure is found in a cast Ti-6Al-4V alloy crafted through the investment casting method. This method stands out

as an exemplary technology for the production of complicated airplane components. It is well established that the fatigue characteristics of titanium alloys hinge on various factors, including surface defects, microstructures, and crystallographic textures **[24], [25]**.

Although investment cast components frequently contain numerous internal cast defects, such as micropores, these defects can typically be rectified through a hot isostatic pressing (HIP) process. Furthermore, fatigue properties are subject to the influence of microstructural elements, such as the size and morphology of β grains, colonies, and α platelets, as substantiated by various research studies **[25]**.

2.6. Additive Manufacturing

2.6.1. Basic Information About Additive Manufacturing

In the 1980s, the introduction of rapid prototyping (RP) marked a pivotal moment in manufacturing technology. RP allowed for the creation of 3D solid parts directly from computer-aided design (CAD) data, revolutionizing the design and production process. Building upon RP techniques, the University of Texas showcased the first additive manufacturing (AM) method in 1986 **[26], [27]**.

According to ASTM F2792-12a **[28]**, AM is described as a method that combines materials to construct objects based on 3D model data, often employing a layer-by-layer approach. This method stands in contrast to traditional subtractive manufacturing methodologies. The thickness of each layer plays a crucial role in determining the final shape and quality of the fabricated object. Thinner layers contribute to creating parts that closely resemble those produced through traditional manufacturing methods **[29]**. Nevertheless, the layer thickness in AM can be influenced by various factors, including thermal inputs and heat sources. Production parameters differ significantly across various material types in the current AM technology context. As a result, commercialized AM machines and the associated process requirements exhibit notable variations depending on the manufactured materials **[29]**.

The versatility of AM is evident in its capacity to fabricate parts from polymers, ceramics and metals. As illustrated in **Figure 2.10 [30]**, a range of AM techniques addresses different materials. Polymers are shaped using methods such as

stereolithography (STL) and ink jetting, while ceramics find form through processes like binder jetting, ink jetting and stereolithography. Metal parts, on the other hand, are realized through techniques like directed energy deposition and powder bed fusion, showcasing the breadth of AM's capabilities **[27], [28]**.

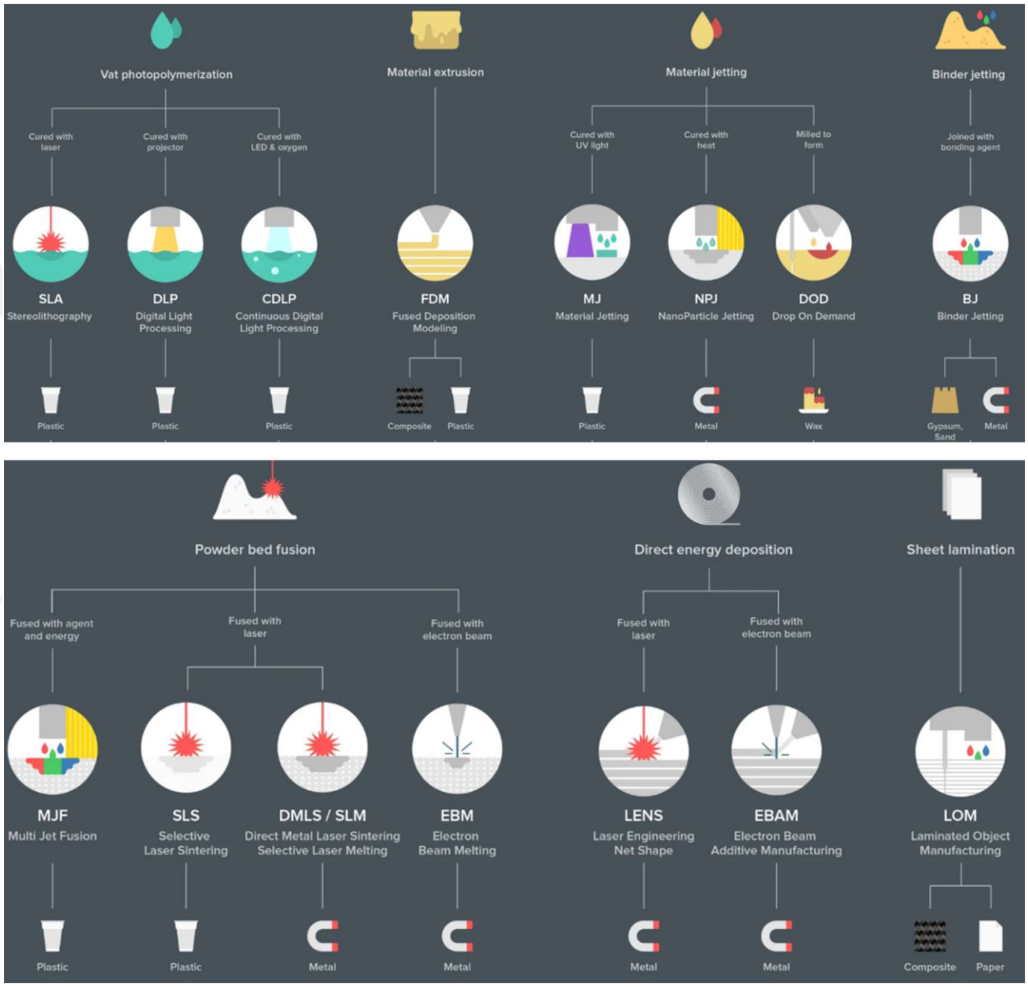

Figure 2.10 : Visual demonstration of AM production methods. Adapted from **[30]**.

2.6.2. The Benefits of AM Method and It's Applications

Additive manufacturing (AM) is currently in a dynamic growth phase, and its far-reaching implications are poised to start a new era of industrial transformation. AM's primary advantage lies in its capacity for structural flexibility, enabling the creation of exceptionally intricate components within a single manufacturing step. In contrast, conventional manufacturing techniques often necessitate multiple sequential stages to

create complex parts. Employing AM, as opposed to conventional methods, reduces the number of required processes **[31], [32]**.

This opportunity for design freedom enables the cost-effective fabrication of distinctive products at lower production volumes. As production volumes rise, traditional manufacturing techniques usually become more economical. Conversely, AM comes into its own when production volumes are lower, and there is a need for constant design variations. In such scenarios, AM can yield significant cost savings potential while also reducing the environmental footprint by minimizing transportation, packaging, and storage requirements. Furthermore, AM is known for its lower energy consumption, which contributes positively to environmental sustainability. The versatility of AM technologies extends across various industries, including aerospace, biomedical, fashion industry, food manufacturing, construction, and more, making them a preferred choice due to their numerous advantages **[26], [27], [33].**

The aerospace sector currently represents 18.2 % of the overall AM market and holds significant promise for the future. Within this industry, aerospace components must meet specific criteria, including intricate geometries, difficult-to-machine materials, a high material utilization ratio, and the requirement for customized production. Aerospace manufacturing frequently employs advanced and sometimes expensive materials like nickel-based superalloys, titanium alloys, ultra-high-temperature ceramics, and high-strength steel alloys. However, these materials pose challenges regarding production efficiency and generate substantial waste, in some cases up to 95 % of the material. Moreover, the aerospace industry features low-volume production needs and continually changing part designs. AM technologies offer a solution by reducing material waste during manufacturing and providing an economical means to fabricate highly complex shapes **[34], [35]**.

The scope of AM is experiencing continuous expansion, with its layer-by-layer fabrication approach holding significant promise in biomanufacturing. Specific domains such as dentistry and the creation of implants, where tailored anisotropic properties are often required, stand out as prime beneficiaries of AM technology. One particularly important application of AM in the medical field is in the production of implants. These implants are meticulously customized to align with individual patients' unique needs and specifications, making AM an invaluable tool for their fabrication

[36]. For dentistry, AM plays a pivotal role in producing splints, models, and precision drill guides. Furthermore, AM has emerged as a pivotal technology for developing artificial tissues and organs. Additionally, it facilitates the generation of highly detailed 3D models of human organs, aiding in the comprehension of complex human anatomy. Forecasts indicate that the market for AM in biomanufacturing is poised to achieve a value of 26 billion U.S. dollars by 2022 **[37], [38]**.

The fashion industry has witnessed substantial growth, partly due to the highly automated processes facilitated by AM technology. Integrating sophisticated automation techniques has enabled the precise and accurate manufacturing of complex fashion products. This level of precision is pivotal in meeting the demands of today's market, where higher customer satisfaction is a central factor **[28]**. Industry giants such as Nike have embraced AM in their manufacturing operations. Nike utilizes AM to craft lightweight plates essential for its Vapour Laser Talon and Vapour High Agility football cleats **[39], [40]**. Contemporary fashion designers increasingly view additive manufacturing as a transformative technique, enhancing both product quality and design. It empowers customers to personalize their products in distinctive and individualized ways **[41]**. The continuous advancement of AM technology has enabled designers to create materials resembling breathable fabrics, producing lightweight and flexible fashion items. This evolution in AM techniques contributes significantly to the innovation and versatility of the fashion industry **[42]**.

The concept of additive food manufacturing diverges significantly from traditional robotic manufacturing processes. In this innovative approach, complex shapes of varying sizes are meticulously constructed layer by layer and subsequently bound together through chemical reactions or phase transitions, setting them apart from conventional manufacturing methods. Additive food manufacturing offers a level of customization that allows users to select shapes, flavors, and ingredients tailored to their specific preferences and requirements **[43], [44]**. The development of additive food manufacturing printers is currently driven by specific needs and applications, such as using laser technology to craft intricate additive chocolate creations **[45]**.

Since 1997, the construction industry has gradually embraced AM processes. Despite its clear advantages over conventional methods, such as reduced on-site risks, expedited production, decreased emissions, and minimized material waste, the integration of this technology into construction has progressed relatively slowly. To

date, AM techniques have been successfully applied in the construction sector for a wide range of purposes. These include the construction of intricate structures, basic wall assemblies, curved surface designs, manufacturing of concrete beams, development of architectural prototypes, fabrication of bridge components, and the construction of residential properties, including houses and villas **[46], [47]**.

2.6.3. Workflow of the AM Method

AM techniques typically follow a layered approach for component production. **Figure 2.11** illustrates a general production flow diagram for AM **[48]**. The process starts with the generation of a CAD model representing the desired component. This CAD model is then transformed into an STL (Stereolithography) file, which digitally dissects the 3D model into multiple layers. Following this, the part is built layer by layer using an AM method. After production, the component is removed from the build platform. Several post-processing steps, such as heat treatment, cleaning, or grinding, are employed, depending on the specific AM techniques employed **[49]**.

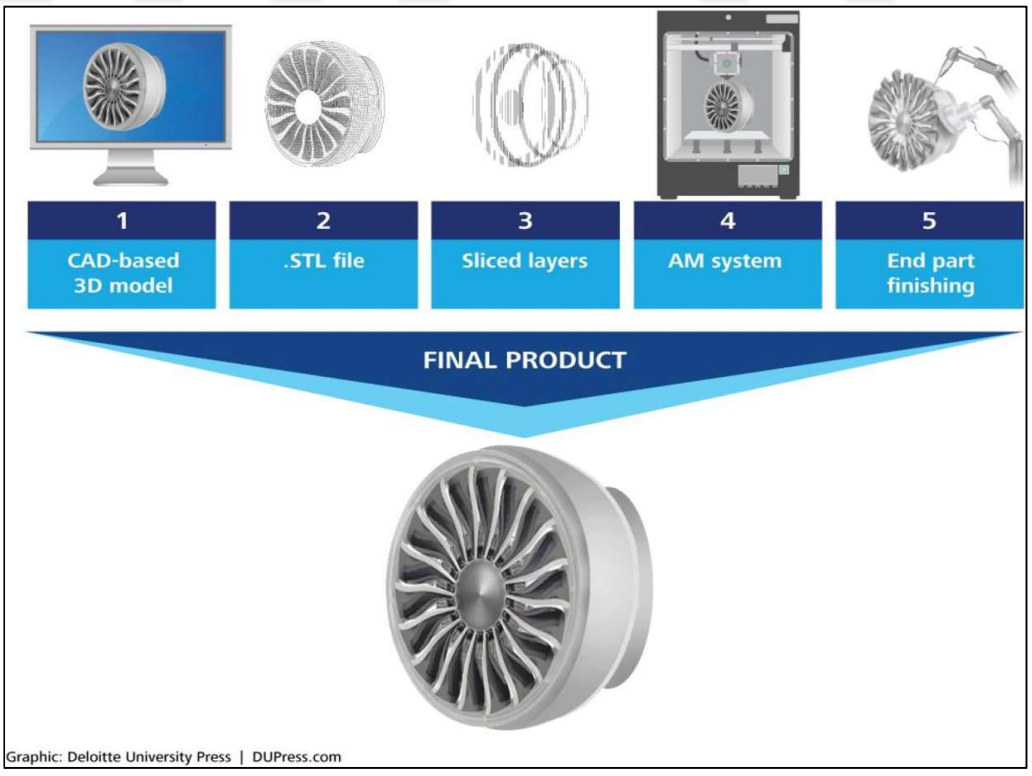

Figure 2.11 : Demonstration of the steps in the AM process. Adapted from **[48]**.

2.6.4. Types of the Metal AM Method

AM techniques employ either an electron beam or a laser beam as their energy source for building parts, using raw materials in wire form or powder. When using powdered materials, the electron beam or laser beam can be precisely focused on a stationary powder bed with a predefined layer thickness on a build platform. Alternatively, a nozzle near the laser beam may be utilized to add powder or powder mixtures onto the platform. These techniques are referred to as the powder bed fusion process (PBF) and the directed energy deposition (DED) process, respectively **[50]**. These methods involve the partial or complete melting of metallic materials to create solid components which can range from fully dense to porous structures. Alternatively, other methods such as direct metal writing, binder jetting, cold spraying, and friction stir welding can be employed for the fabrication of metal components **[34], [51], [52]**.

2.6.4.1. Powder Bed Fusion (PBF) Technique

Powder Bed Fusion (PBF) employs high-energy sources, namely lasers and electron beams, to achieve the fusion or sintering of metallic powders. This intricate process is initiated by the precise deposition of a fine metal powder layer on the build plate, followed by subsequent selective melting guided by CAD data. As the procedure is repeated, the build platform descends incrementally in the z-direction, and this sequence iterates until the 3D component attains its final form. Each layer of the produced part seamlessly fuses together, facilitated by the power source's ability to penetrate beyond a single layer **[53]**.

For Metal AM, the PBF method falls into two primary categories: Electron Beam Melting Powder Bed Fusion (EB-PBF) and Laser Powder Bed Fusion (L-PBF), distinguishing them based on the energy source utilized. Critical to the success of this process is the requirement that metal powders maintain a spherical shape and possess an optimized particle size distribution, enhancing their flow and characteristics. Throughout the manufacturing process, oxidation is meticulously managed by either introducing inert gases like nitrogen (N) or argon (Ar) or by creating a vacuum environment **[54], [55]**.

EB-PBF represents an advanced AM technique characterized by the utilization of a high-energy electron beam to systematically melt layers of metal powder, enabling the

creation of fully dense solid components **[56]**. The origins of EB-PBF as a manufacturing technique can be traced back to its development at Chalmers University in Sweden, with subsequent commercialization in 2001 through the establishment of ARCAM AB company **[50]**. **Figure 2.12** serves as a comprehensive visual representation of the primary components of the EB-PBF machine **[57]**.

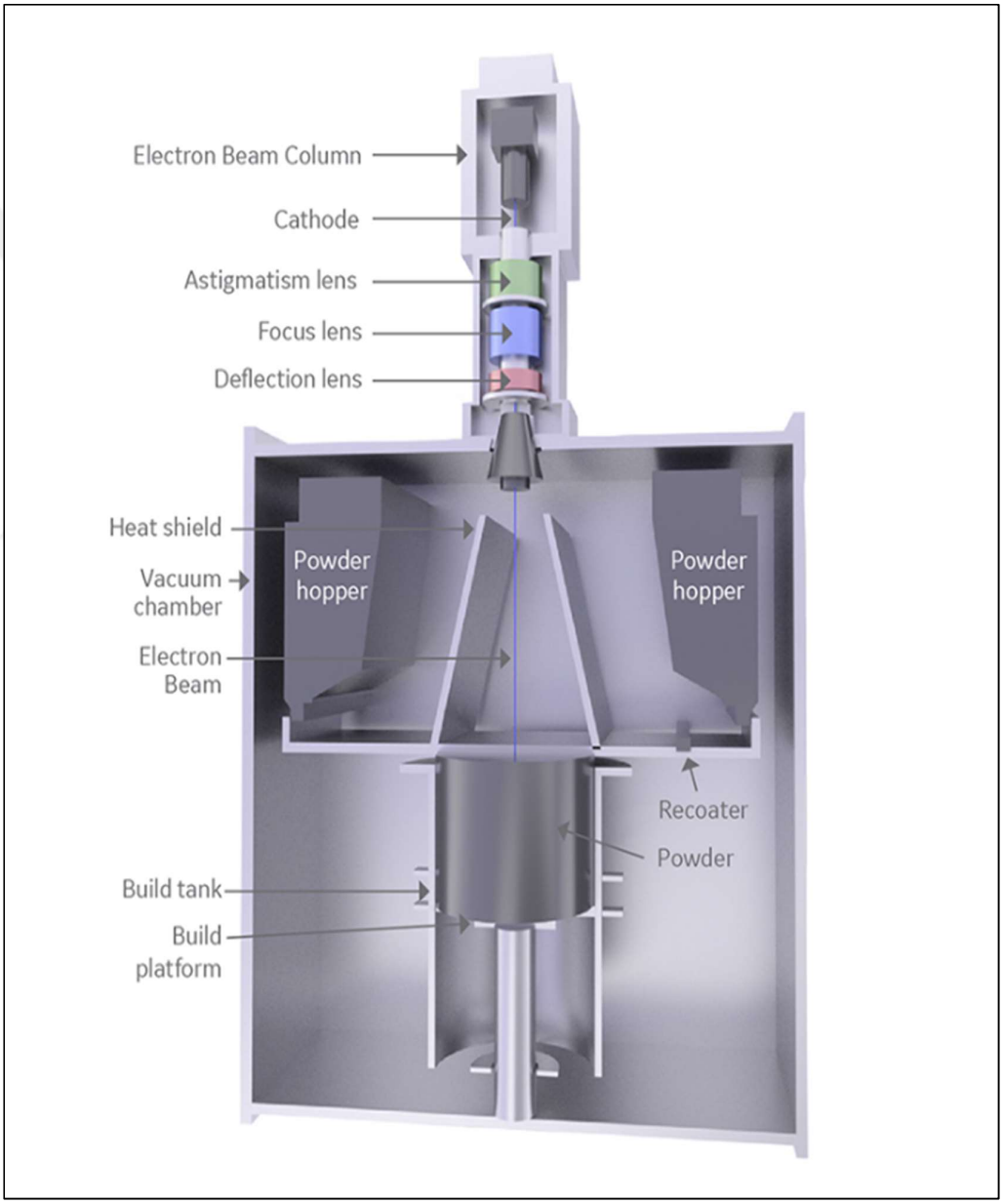

Figure 2.12 : Demonstration of the EB-PBF machine layout. Adapted from **[57]**.

The necessity for a vacuum environment in the manufacturing process arises from the electron beam's inherent requirement for a vacuum, effectively reducing impurities

and ensuring the integrity of oxygen-sensitive materials. This method often incorporates a preheating stage where the electron beam is rapidly scanned across the powder before the layer is melted, thereby contributing to the minimization of residual stresses within the fabricated components. Remarkably, the mechanical properties of components produced via EB-PBF can closely resemble to those of traditionally cast materials, the efficiency and potential advantages of this manufacturing method makes this method superior compared to conventional methods. This method contributes to significantly accelerated manufacturing processes because of faster scanning and the ability to melt thicker layers of powder **[56]**.

L-PBF technology is a leading method in metal AM, characterized by its use of high-powered lasers to selectively melt and solidify individual layers of metal powder **[58]**, **[59]**. In this process, a supply of metal powder is delivered and evenly distributed onto a designated platform, where it undergoes controlled melting and solidification in alignment with the CAD design specifications. The precision of this procedure depends on a range of user-selectable parameters, including laser scanning strategies, layer thickness, inert atmosphere conditions, gas flow rates, and various other variables, all of which must be meticulously optimized to suit the specific material and system being utilized **[58]**.

L-PBF stands out as the prevailing method within the realm of metal AM, offering a multitude of machine options from various manufacturers and a vast spectrum of compatible materials. L-PBF machine layout and working principle as shown in **Figure 2.13 [60]**. These materials encompass a diverse range, including aluminum alloys, steel alloys, copper alloys, nickel and iron-based superalloys, precious metals, refractory metals, titanium alloys, and an extensive array of others **[58]**. This method is renowned for its ability to fabricate fully dense components with exceptional precision, often within a relatively short timeframe **[61]**. However, it is important to note that the inherent sophistication of the L-PBF process can translate into higher manufacturing costs. Consequently, L-PBF finds its most optimal utility in industries prioritizing high-value components and where enhanced performance can ultimately lead to cost reductions, with the aerospace sector serving as a prime example **[58]**.

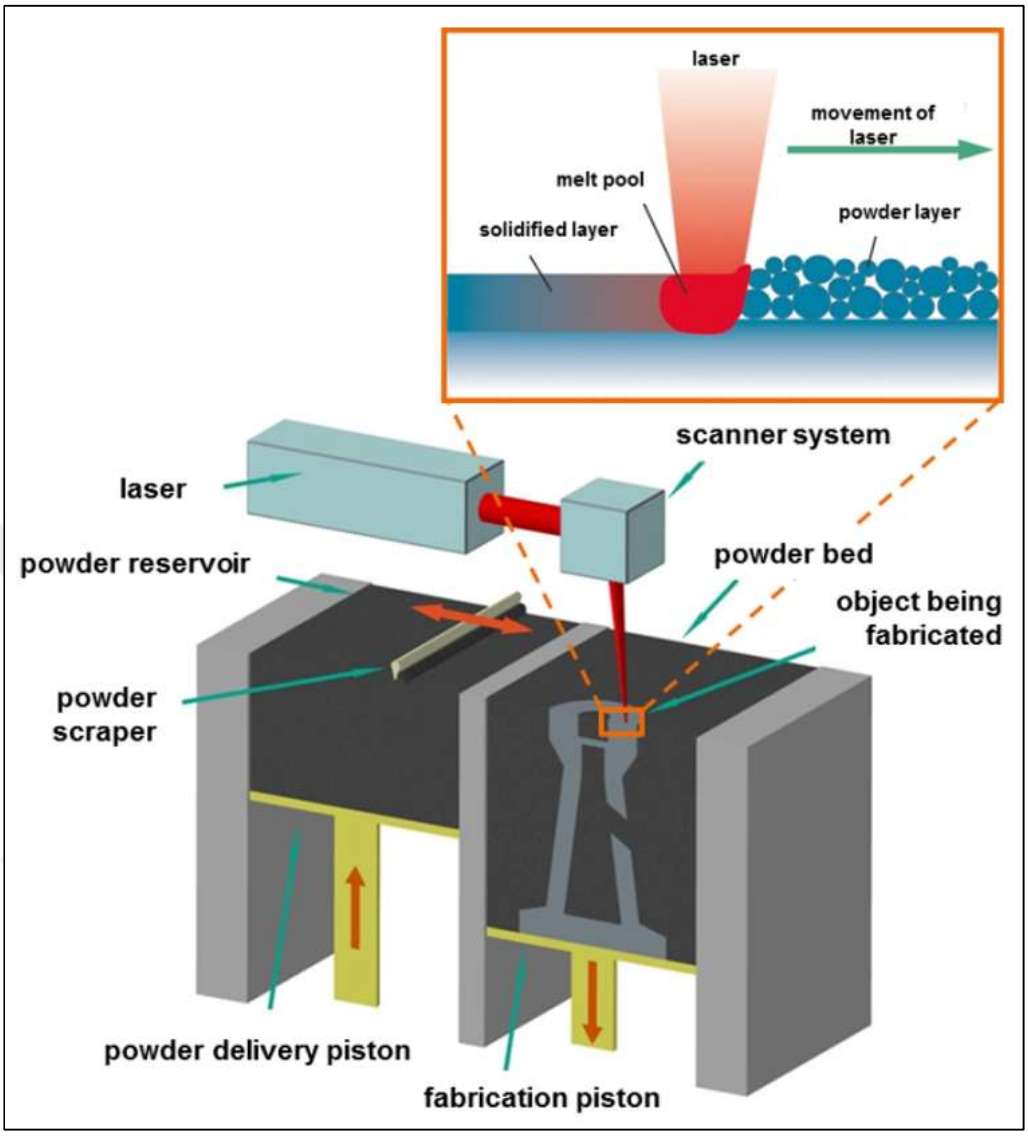

Figure 2.13 : Visual demonstration of the L-PBF machine layout and working principle. Adapted from **[60]**.

Significant distinctions emerge from the operating principles of EB-PBF and L-PBF due to their energy sources, as specified in **Table 2.3 [62]**. Within the L-PBF process, the heating mechanism relies on the absorption of laser beams by powder particles, resulting in their heating. Conversely, EB-PBF utilizes electron energy conversion into powders for the necessary heating. Notably, EB-PBF achieves a notably higher temperature within the powder bed than L-PBF, enabling the rapid fabrication of materials characterized by high melting points. This elevated temperature in EB-PBF results in a more extensive and diffusive heat input at a slower cooling rate than the L-PBF process. The rapid cooling in L-PBF results in the development of smaller grain

sizes in the microstructure. Conversely, larger heat input within a given time frame can form non-equilibrium phases. Furthermore, EB-PBF necessitates a powder bed with conductive properties, limiting its application to the production of conductive materials such as metals. In contrast, L-PBF offers a more versatile application range, as it can be employed with any material capable of absorbing the laser wavelength's energy, including but not limited to metals, ceramics and polymers **[63]**.

Table 2.3: L-PBF and EB-PBF differences.

Attribute	**L-PBF**	**EB-PBF**
Energy Source	Laser	Electron beam
Production Environment	Inert gas	Vacuum
Powder Size	Fine	Coarse
Surface Quality	High	Low
Residual Stress	High	Low
Mechanical Results (Same Material)	High	Low
Waste Material Ratio	High	Low
Materials	Polymer, metal, ceramic	Metals

2.6.4.2. Directed Energy Deposition (DED) Technique

The directed energy deposition (DED) technique involves the local deposition of raw material. This deposition is achieved by introducing powdered material or directly feeding wire feedstock into a meltpool. The meltpool itself is generated through the application of various energy sources such as laser beams, electron beams etc. **[64]**. A significant advantage within DED systems lies in their incorporation of multiple powder feeders, each capable of individually controlling the powder feed rate. This characteristic proves to be of exceptional utility in the context of fabricating structures composed of multiple materials, thereby enhancing versatility in the manufacturing process **[65]**. This technology extends to its implementation in multiaxial machines,

endowing them with the capability for precise 3D positioning **[66]**. DED technologies are suitable for manufacturing large parts and repairing critical components such as turbine blades, engine combustion chambers, compressors, blisks etc., owing to the versatility in orientation and flexibility **[67], [68]**.

A primary challenge associated with DED is the residual stresses induced by non-uniform thermal expansion and contraction during manufacturing. These thermal fluctuations can trigger distortion and, in turn, the formation of cracks, compromising the structural integrity of DED-produced parts. The other concern is the surface quality of manufactured DED components **[69], [70]**.

Laser beam-based DED systems exhibit versatility by using either wire or powder feedstock for the AM process. A visual demonstration of the laser beam-based DED technique is provided in **Figure 2.14 [71]**, offering a visual insight into its intricacies. This approach allows the system to have one or more nozzles to increase efficiency, and it allows the laser and powder spray nozzles to move in tandem as needed. The effectiveness of the process depends on several critical parameters, including the relative velocity between the laser and substrate, laser beam diameter, laser power output, hatch spacing, powder feeding rate, and the selected scanning strategy. Furthermore, when working with reactive metals, the incorporation of a fully inert chamber is mandatory, serving as a safeguard for both operational safety and the integrity of the additive manufacturing process **[72], [73]**.

Metal wire is used as feedstock in electron beam-based DED systems, which melt it in a vacuum using an electron beam. A schematic representation of the electron beam-based DED technique is provided in **Figure 2.15 [74]**. These systems reach up to 9 kg/h in deposition rate. The utilization of electron beams, known for their superior energy levels compared to lasers, affords a distinct advantage in achieving higher precision, mainly when operating at lower deposition rates and working with thinner layers **[53], [73]**.

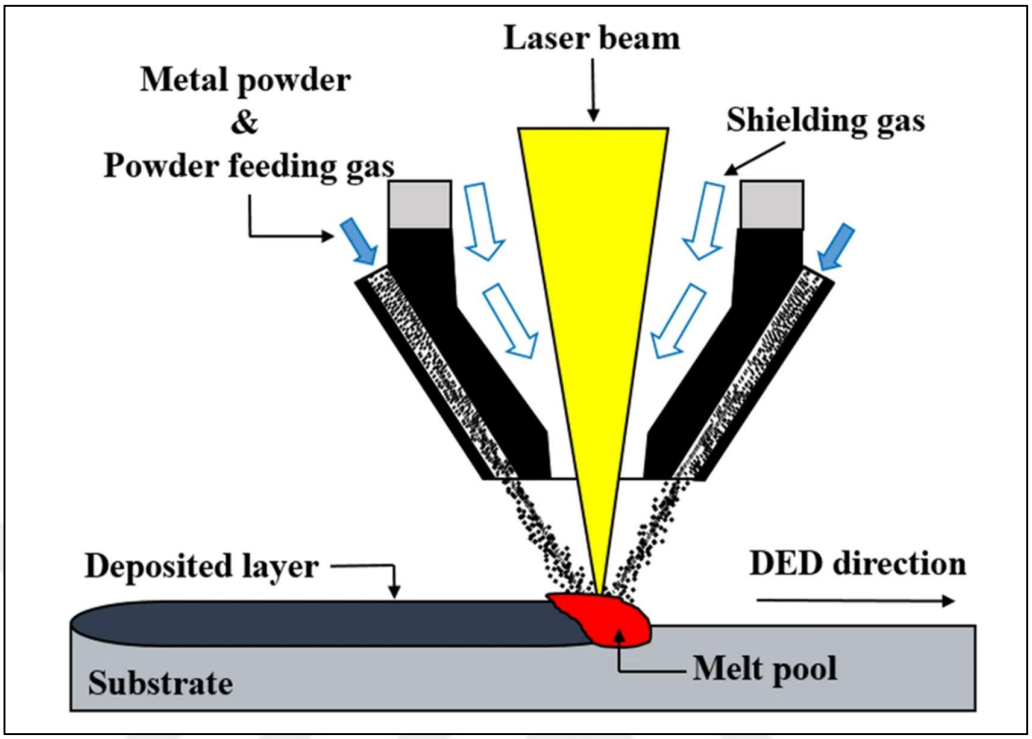

Figure 2.14 : Visual demonstration of the laser beam DED machine layout and working principle. Adapted from **[71]**.

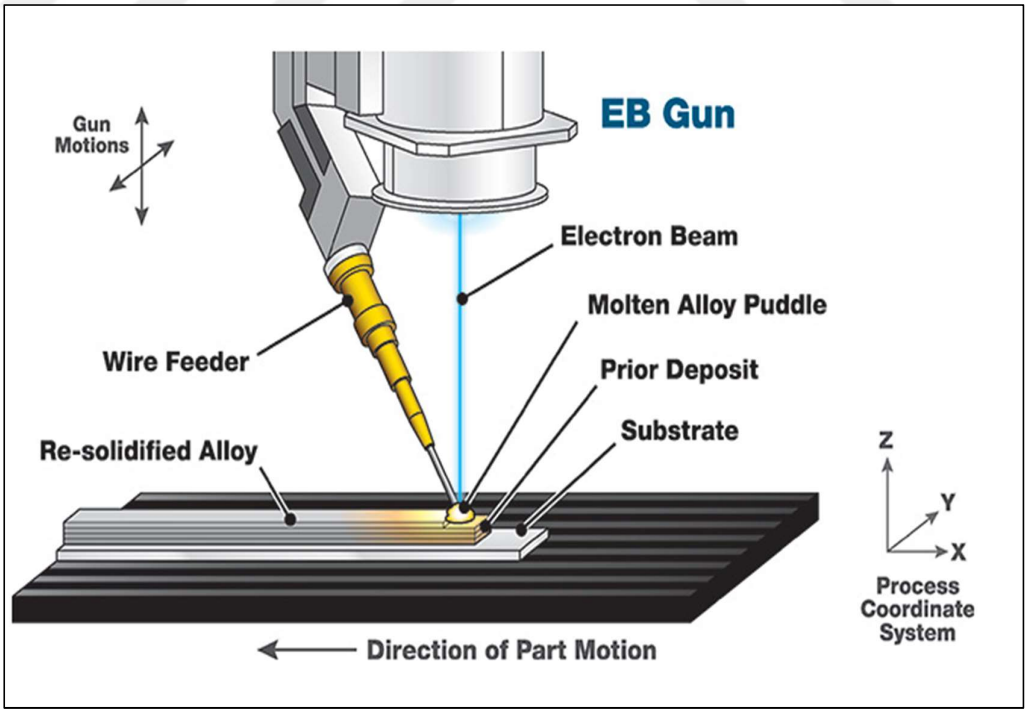

Figure 2.15 : Visual demonstration of the electron beam DED machine layout and working principle. Adapted from **[74]**.

2.6.5. Ti-6Al-4V Production by AM Method

Ti-6Al-4V alloy components can be manufactured using conventional techniques like forging, powder metallurgy, and casting. A combination of these methods is often required to produce a single part. However, conventional manufacturing methods struggle to produce intricate, highly precise geometries cost-effectively, generating significant waste material. AM methods have transformed this industry by enabling the creation of complex Ti-6Al-4V alloy parts with minimal waste in a single step. For manufacturing Ti-6Al-4V alloy components with precision and efficiency, there are several metal AM methods **[1], [75]-[77]**. Although many AM techniques can be utilized to produce complex Ti-6Al-4V alloy components, we will focus on EB-PBF AM method in this section.

In the literature, there are many studies examining the mechanical and fatique properties of Ti-6Al-4V alloy that produced by investment casting and different AM methods. Some of these studies are given in the following section.

Gong et al. **[78]** examined the impact of flaws on the mechanical characteristics of Ti-6Al-4V components, which are manufactured using the EB-PBF and L-PBF processes. The outcomes of their research revealed that defects were generated during the L-PBF process due to low energy input, resulting in compromised mechanical properties. Interestingly, defects were also observed in specimens with excessive energy input during L-PBF, although their detrimental impact was less than those stemming from lower energy conditions. For the method of EB-PBF, large defects were observed when the manufacturing procedure strayed from the prescribed optimal process parameters, leading to an evident deterioration in mechanical properties. Samples of Ti-6Al-4V produced through both the L-PBF and EB-PBF techniques displayed similar levels of fatigue strength, tensile ductility and hardness. However, it was noted that L-PBF performed slightly better than EB-PBF in yield and tensile strength.

Rafi et al. **[79]** conducted a comprehensive analysis comparing the mechanical properties and microstructures of Ti-6Al-4V components fabricated using EB-PBF and L-PBF techniques. In terms of microstructure, L-PBF produced Ti-6Al-4V parts with martensitic α' microstructures, while EB-PBF produced parts characterized by an α phase with a β phase separating the alpha lamellae. L-PBF-produced parts reached the highest tensile strength attributed to the presence of the martensitic α'

microstructure. At the same time, the EB-PBF-produced parts exhibited superior ductility primarily due to the lamellar α phase. This difference in microstructure also led to significant differences in fatigue performance, with EB-PBF parts exhibiting a fatigue limit of 340 MPa. In comparison, L-PBF specimens reached a very high fatigue limit of 550 MPa.

Chern et al. **[80]** investigated the fatigue characteristics of Ti-6Al-4V alloy components manufactured through EB-PBF and subjected to various post-processing treatments. They studied the effects of annealing heat treatments and stress relief on the microstructure and mechanical characteristics of these components both before and after HIP and machining. Their results showed that these treatments often led to microstructure coarsening, which did not enhance fatigue resistance. To improve fatigue resistance in EB-PBF parts, they recommended using a combination of HIP and machining as the most effective approach for achieving the desired fatigue performance enhancement.

Wycisk et al. **[81]** looked at the as-built and polished states, as well as orientations at both vertical and 45° "tilted" positions, in order to study the high cycle fatigue behavior of additively manufactured Ti-6Al-4V components. The research findings indicated that the build orientation did not exert a significant impact on fatigue performance. However, there was a substantial difference in endurance limits between the as-built and polished specimens, with the as-built specimen exhibiting an approximately 60% lower endurance limit than the polished one. Additionally, as stresses got closer to the endurance limit, the fatigue performance of the polished components varied more, which was explained by the start of fatigue cracks at both internal and external flaws like pores. In contrast, the as-built components exhibited a different behavior, with all cracks initiating exclusively from the rough surface.

Edwards et al. **[82]** examined different surface conditions, including as-built, machined, and machined plus shot penned, in both horizontal and vertical structural directions while examining the fatigue characteristics of Ti-6Al-4V components made using the EB-PBF process. Their study revealed that the fatigue performance is significantly constrained by both the rough as-built surface and the presence of internal porosity. The fatigue behavior of the machined specimens did not differ significantly from the as-built specimens. This similarity was attributed to the fact that machining exposed internal pores, effectively transforming them into crack initiation sites.

Additionally, the study discovered no obvious distinction in fatigue behavior among the various construction orientations, despite the small size of the data set. The impact of internal defects and surface conditions on fatigue behavior was highlighted by the observation that, on average, the fatigue strengths of the additively made specimens were about 80% lower compared with that of the wrought material.

Li et al. **[83]** conducted a comprehensive review focusing on fatigue investigations involving AM Ti-6Al-4V subjected to axial cyclic loading. Their comprehensive analysis highlighted a consistent trend where AM materials exhibited shorter fatigue life compared to their wrought counterparts. This variation in fatigue performance has been attributed to several influential factors, including internal defects, residual stresses, and surface conditions. Fatigue resistance in AM materials was significantly reduced by internal defects, which mostly took the form of porosity and unmelted particles. These defects functioned as stress concentrators, generating notches that contributed significantly to the reduced fatigue performance observed in AM materials when compared to their wrought counterparts.

Eylon **[84]** conducted a study highlighting a significant decrease in the high cycle fatigue strength of cast Ti-6Al-4V alloys. This decrease was closely associated with the presence of coarse micropores within the material. However, Eylon's research demonstrated a potential way to improve via the application of HIP. In the field of high-cycle fatigue, the life of a material is tied to the initiation and propagation of fatigue-induced cracks. When internal defects are minimal, most of the fatigue life is consumed during the initial stages of crack formation. Therefore, it becomes a necessity to find these crack initiation sites and clarify the mechanisms that lead to the cracking process.

Pilchak et al. **[85]** investigated the impact of particles including yttrium (Y) on the microstructure and fatigue characteristics of HIP Ti-6Al-4V and investment casting specimens. Their research covered high-cycle fatigue evaluations combined with a detailed fractography analysis. Conducting high cycle fatigue tests and a detailed fractography analysis, it became evident that Y-containing particles had a negligible impact when contrasted with the dominant factors, namely the substantial colony size and resulting shear length found within the cast material.

Yoder et al. **[86]** made a significant discovery concerning the influence of oxygen content variation within Ti-6Al-4V alloys. They observed a direct correlation between oxygen content and the size of primary beta grains and Widmanstätten packets, which, in turn, had a substantial impact on the rate of fatigue crack propagation. However, beta-annealed Ti-6Al-4V alloys exhibited a wide range of microstructures with varying oxygen levels, resulting in Widmanstätten sizes ranging from 17 to 38 μm and primary beta grain sizes ranging from 214 to 844 μm. Therefore, it was not possible to definitively establish an interaction regarding oxygen content and fatigue crack growth rates despite investigations. It's also critical to remember that the test environment has a big impact on fatigue fracture propagation rates in addition to the titanium alloy's internal oxygen variation.

In the study conducted by Hornberger et al. **[87]**, It was observed that titanium alloys were subjected to a reactive process with oxygen from the surrounding air, resulting in the formation of oxide layers on the specimen's surface. These surface oxides serve as focal points for stress concentration and ultimately start the development of fatigue cracks. Over time, this phenomenon results in a significant reduction in the fatigue life of the material.

2.7. Importance of Ti Alloy in Aerospace Applications

Weight is an important criterion in aircraft design since it is directly related to fuel consumption. Compared to metals like steel, Titanium's lower density presents an applicable option for achieving weight savings in design components. Furthermore, titanium demonstrates remarkable strength retention even under high temperatures, a characteristic unmatched by other lightweight metals such as aluminum. Despite titanium having a density approximately 60 % higher than aluminum, its dominance in selection criteria is attributed to its superior heat resistance coupled with a favorable lower density profile **[8]**.

Within the aerospace industry, where operational excellence under difficult conditions is essential, titanium is emerging as the material of choice, particularly for components subjected to high thermal stresses. Because of its excellent corrosion resistance, moderate thermal expansion, lack of fracture at low temperatures, capacity to reduce

weight, and performance in heat-resistant environments, titanium alloys find extensive application in aerospace **[88]**.

The diagram shown in **Figure 2.16 [89]** and **Figure 2.17 [90]** provides a detailed overview of the wide range of aircraft and engine components manufactured from titanium alloys. This illustration highlights the significant contribution of titanium to aerospace engineering, where its different properties are utilized to optimize performance and ensure the reliability of vital systems **[2], [8]**.

Ti alloys are used for the parts that work at low and medium temperatures. As can be seen in **Figure 2.16** and **Figure 2.17**, Ti alloys are used in many parts of the engine and aircraft in the aerospace industry. For example, hydraulic tubing, landing gear, frames of cockpit windows, loading doors, rails for seats, rings for engines, discs, fan blade, blisk, front frame, compressor blade, crossbars, reinforcement profiles, wing flap rails, and turbine covers etc. **[2]**.

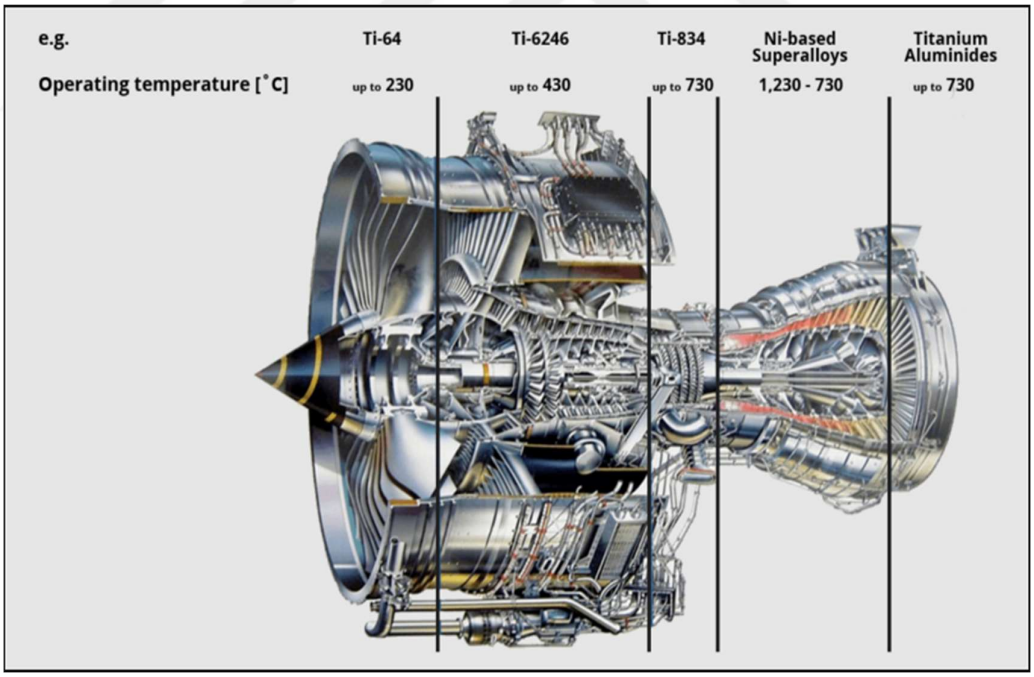

Figure 2.16 : A cross section of a Trent 900 aero engine, Rolls Royce. Adapted from **[89]**.

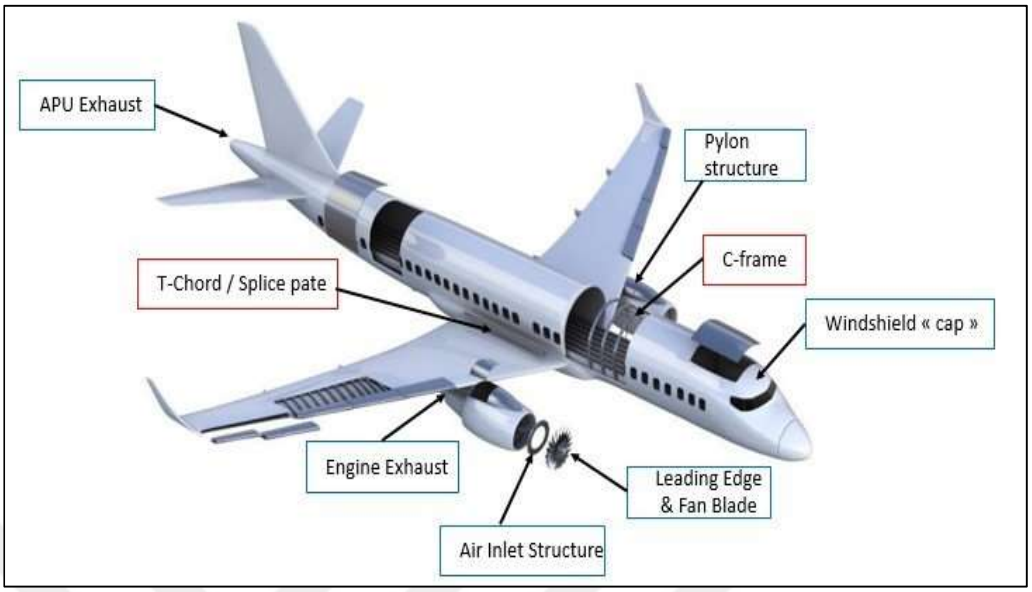

Figure 2.17 : Demonstration of titanium alloy parts in an airplane. Adapted from **[90]**.

3. EXPERIMENTAL PROCEDURE

In this part of the thesis, general information about the production details of the fatigue test specimens produced by EB-PBF and IC methods, the post processes (machining, annealing, and HIP based on requirements) applied to the test specimens, and the test equipment used for the tests are discussed.

3.1. Specimen Production by EB-PBF

The material, production equipment, process parameters, production orientation and post processes to the Ti-6Al-4V alloy fatigue test specimen that produced by EB-PBF method are given in the following subheadings.

3.1.1. Material

Generally, Ti-6Al-4V grade 5 powders were used to create fatigue test specimens of Ti-6Al-4V alloy when the literature studies were examined. The grade 5 powder conforms to ASTM F2924-14 and its chemical properties are given in **Table 3.1** below. The powder size of Ti-6Al-4V is within the range of about 45 to 106 μm **[91]-[92]**.

Table 3.1 : Composition of Ti-6Al-4V grade-5 powder and ASTM F2924-14.

Element	Chemical Composition (wt. %)	
	ASTM F2924-14 (AM)	**Ti-6Al-4V Grade-5 Powder**
Al	5.50 to 6.75	6
V	3.50 to 4.50	4
Fe	0.30 max.	0.1
O	0.20 max.	0.15
C	0.08 max.	0.03
N	0.05 max.	0.01
H	0.015 max.	0
Titanium	Balance	Balance

3.1.2. Production Equipment and Build Orientations

When the studies are examined, fatigue test specimens are generally produced using AM machines such as ARCAM EBM A2X and ARCAM EBM Q20plus, as shown in **Figure 3.1** and **Figure 3.2**. As shown in **Figure 3.3**, the specimens are mostly produced in two different production orientations, vertical (Z) and horizontal (XY) **[91]-[92]**. It is crucial that the production parameters remain the same in order to see the impact of the production orientation.

Figure 3.1 : A visual of the ARCAM EBM A2X production machine. Adapted from **[91]**.

Figure 3.2 : A visual of the ARCAM EBM Q20plus production machine. Adapted from **[91]**.

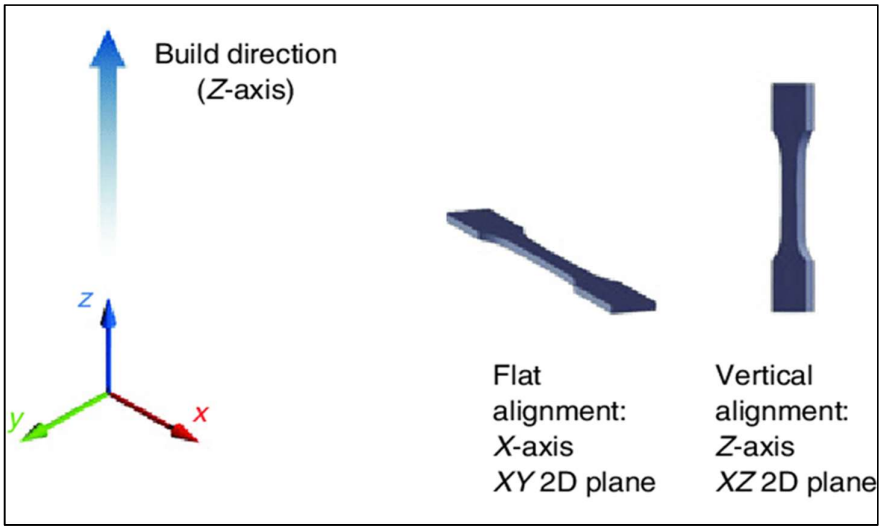

Figure 3.3 : Schematic demonstration of building orientation. Adapted from **[92]**.

Figure 3.4 displays the Z-oriented specimen's visual representation, which is parallel to the manufacturing orientation, and **Figure 3.5** displays the XY-oriented specimen's visual representation, which is perpendicular to the manufacturing orientation.

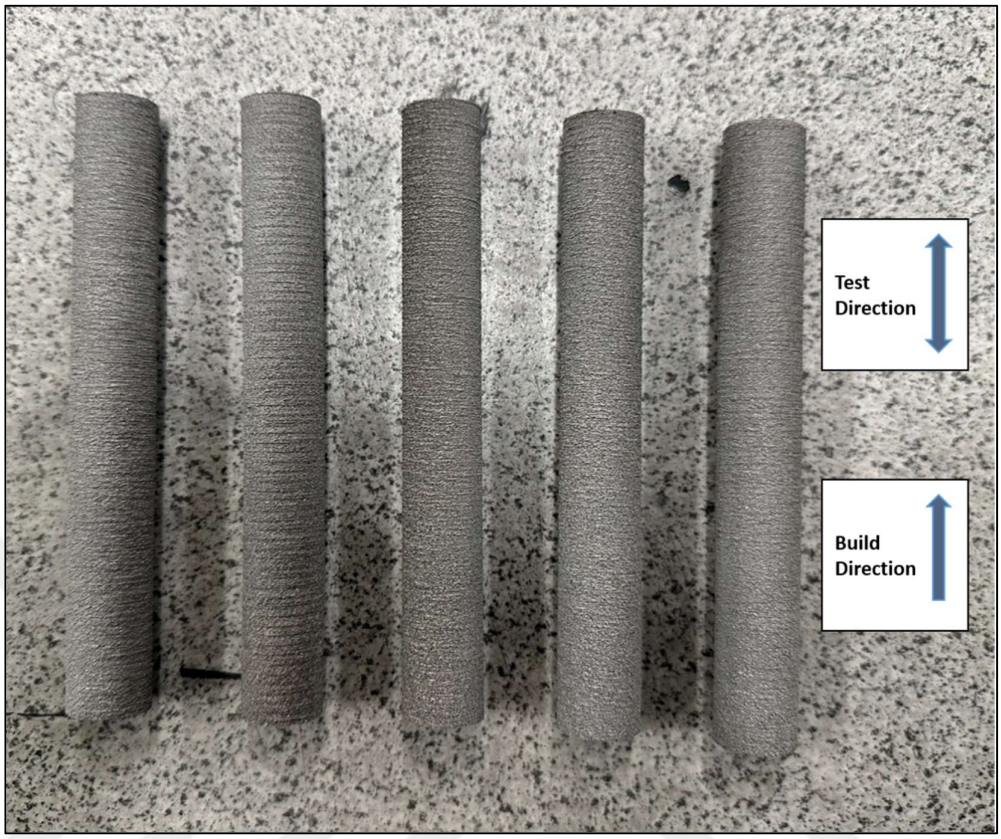

Figure 3.4 : A visual representation of Z-oriented specimens.

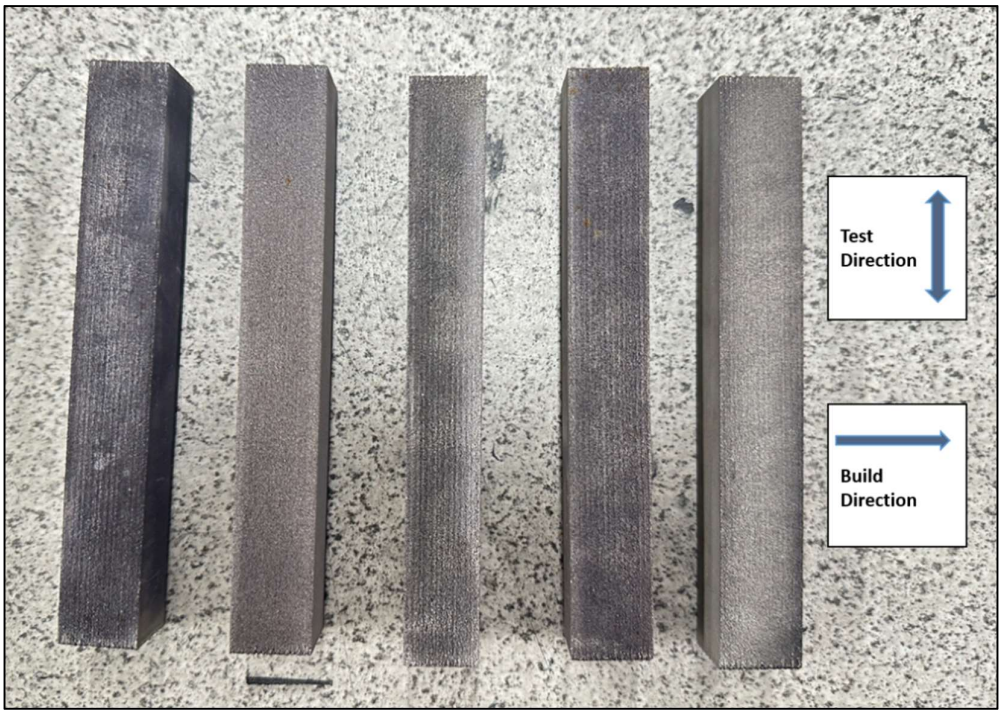

Figure 3.5 : A visual representation of XY-oriented specimens.

3.1.3. Process Parameters

Table 3.2 lists a few of the EB-PBF process parameters that are used in the ARCAM A2X and are typically supplied by the machine supplier for the production of the samples.

Table 3.2 : Process parameters of the EB-PBF.

Process Parameter	Value	Unit
Applied Voltage	60	kV
Layer Thickness	0.05	mm
Speed Function	45	
Scan Length	45	mm
Focus Offset	25	mA
Max. Current	35	mA
Reference Current	12	mA
Min. Current	3	mA
Max. Beam Power	3	kW
Surface Temperature	650	°C
Number of Contours	3	

3.1.4. Post Processes

In cases where the microstructures of the samples produced in both XY and Z directions are at the desired values, only annealing heat treatment can be considered sufficient, and the processes can be carried out accordingly. Common heat treatment methods like annealing are used on additively produced parts to reduce residual stress and increase ductility. The samples are heated to 720 °C for two to four hours while being contained in an inert gas and vacuum environment. They are then cooled in the furnace to below 350 °C. Furnace temperature tolerances of +/- 14 °C for annealing are important for the reliability of the furnace, and care is taken to ensure these values are met. In general, operations are carried out with the furnace that meets this requirement **[93]**.

Electron beam melting tends to provide unsatisfactory surface quality due to the melting pool's elevated temperature. The elevated temperature causes the powders

surrounding the intended contour to sinter onto the surface, leading to the creation of a porous surface. Porous texture has the potential to interfere with the accuracy of test results. To minimize the impact of surface quality, the test specimens are surface treated. This strategic approach also aims to explore the impact of the production direction on the final result.

Tensile tests are performed at room temperature on specimens produced by EB-PBF in order to verify the specimens produced by EB-PBF. **Table 3.3** below displays the requirements and results of the tensile tests for the XY and Z directions. **[94]**.

Table 3.3 : Minimum tensile properties for XY and Z-direction specimens **[94]**.

Minimum Room Temperature Tensile Properties	Specimen Minimum XY Requirements	Test Results of XY Specimen	Specimen Minimum Z Requirements	Test Results of Z Specimen
Tensile Strength (UTS) [MPa]	860	967 +/- 29	860	1023 +/- 21
Yield Strength at 0.2% Offset [MPa]	795	852 +/- 16	795	940 +/- 23
Elongation [% in 4D]	10	19,5 +/- 5	10	10,2 +/- 2

3.2. Specimen Production by Investment Casting

The material, production equipment, process parameters and post processes to the Ti-6Al-4V alloy fatigue test specimen that produced by IC method are given in the following subheadings.

3.2.1. Material

The processes of fatigue test specimens produced by investment casting method based on ASTM 4992 standard have been advanced. The visual representation of the fatigue test specimen produced by investment casting method is shown in **Figure 3.6**. These dimensions are the blank specimen dimensions before machining.

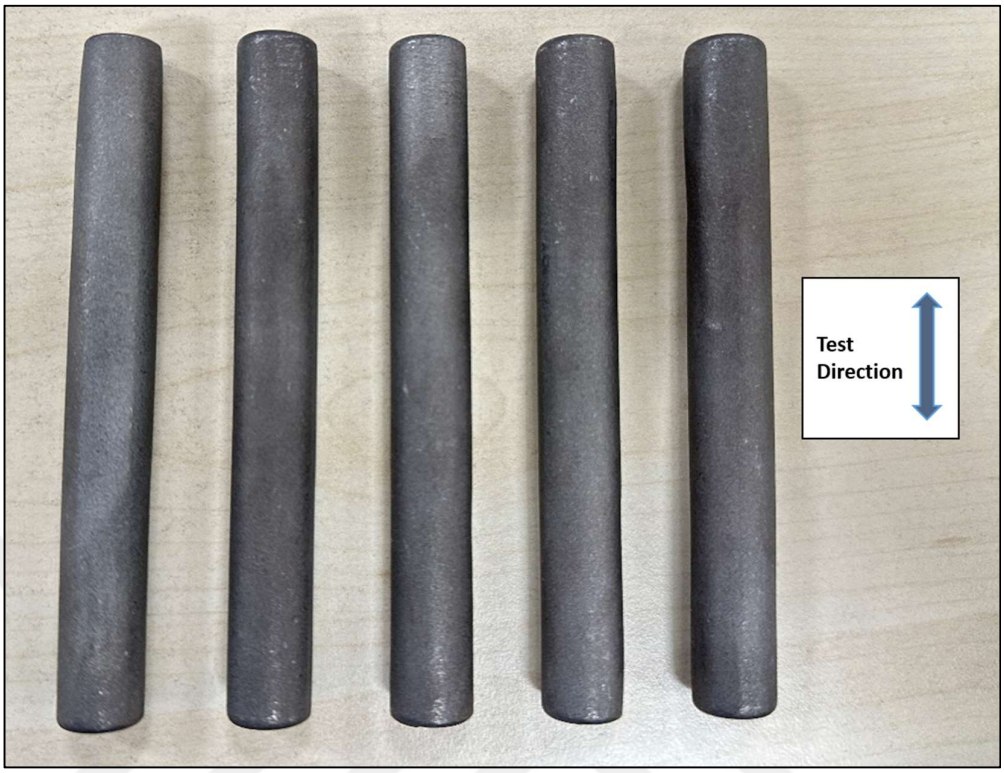

Figure 3.6 : Schematic representation of casting specimens.

Table 3.4 below presents a comparative examination of the cast material's chemical analysis results based on specifications.

Table 3.4 : The elemental composition of Ti-6Al-4V casting specimen and ASTM 4992 standard.

Element	Chemical Composition (wt. %)	
	ASTM 4992	**Test Results of Casting Specimens**
Al	5.50 to 6.75	6.50
V	3.50 to 4.50	3.98
Fe	0.30 max.	0.14
O	0.15 to 0.20	0.179
C	0.10 max.	0.012
N	0.05 max.	0.005
H	0.015 max.	0.0006
Titanium	Balance	Balance

3.2.2. Post Processes

Both HIP and annealing heat treatments can be applied to the specimens manufactured by investment casting method according to their microstructure values. The process parameters of the HIP process are given in **Table 3.5** and the process parameters of the annealing process are given in **Table 3.6 [93], [95]**. Furnace temperature tolerances of +/- 14 °C for HIP and annealing are important for the reliability of the furnace and care is taken to ensure these values. In general, operations are carried out with the furnace that meets this requirement.

Table 3.5 : HIP process parameters as per AMS4992.

Type of the Treatment	Temperature	Pressure	Soaking Time	Cooling procedure
HIP	At selected temperature between 899°C - 954°C within ± 14 °C	100 MPa	180 min ± 60 min	Cool under inert atmosphere in the autoclave to below 427°C

Table 3.6 : Annealing process parameters as per AMS4992.

Type of the Treatment	Temperature (°C)	Duration (hours)	Cooling procedure
Annealing	704 - 843 °C ±14 °C	2-4 hours	Cool in the furnace to below 538 °C.

Tensile tests are performed on the specimens at room temperature to verify the manufactured specimens. The requirements and tensile test results are given in **Table 3.7** below **[95], [96]**. Tensile tests are generally performed in compliance with ASTM E8 and use a tensile rate of 0.005 in/inch/minute (0.005 mm/mm/minute) at 0.2% yield strength.

Table 3.7 : Minimum tensile properties for casting specimens as per AMS4992.

Minimum Room Temperature Tensile Properties	Specimen Minimum Requirements (AMS 4992) Less than 12,7 mm	Test Results of Casting Specimen
Tensile Strength (UTS) [MPa]	861,8	935
Yield Strength at 0.2 % Offset [MPa]	772,2	845
Elongation [% in 4D]	5	9,6

3.3. Fatigue Test of Ti-6Al-4V Specimens

After the test specimens are produced and prepared with EB-PBF and investment casting, fatigue tests are accomplished with a fatigue testing machine. Fatigue tests can be performed after the test specimens are processed in accordance with the standards specified according to ASTM E606 for low cycle fatigue (LCF) and ASTM E466 for high cycle fatigue (HCF). In this study, comparisons of the specimens produced by both production methods in the literature were made both within and between each other **[92], [93]**.

3.3.1. Fatigue Test and Test Equipment

Fatigue is known as a progressive and enduring deterioration in the structural integrity of a material arising from exposure to cyclic or fluctuating stresses. These stresses may have maximum values that either fall below or equal the static yield strength of the material, contributing to localized damage over time **[92], [93]**.

The expected engineering applications of TiAl alloys focus predominantly on components that are subjected to cyclic or fluctuating loads and inherently carry the potential for fatigue failure. When working with TiAl alloys, a careful approach is essential, given their high susceptibility to rupture fracture. Once nucleated, rupture cracks exhibit a rapid rate of propagation under the influence of repeatedly applied loads. This situation emphasizes the critical need to fully understand and consider the fatigue mechanisms in TiAl alloys for comprehensive engineering evaluations. This

necessitates demonstrating how materials can withstand damage from intrinsic or service-related defects. A crucial part of evaluating TiAl alloys involves thoroughly understanding their fatigue and crack growth properties. To explore their performance under cyclic loading, Ti-6Al-4V alloys in different forms, including both cast and additive, underwent comprehensive examination **[92], [93]**.

High cycle fatigue encompasses a significant volume of cycles subjected to elastically applied stress. Typically, high-cycle fatigue assessments extend to 10^7 cycles. Although fatigue strength, also referred to as the endurance limit, refers to the stress threshold that prevents failure, fatigue life is the number of cycles that lead to failure under a certain stress level. The reduced applied stress level is associated with an increased number of cycles to failure. Generally, an increase in static tensile strength corresponds to an elevation in fatigue strength **[92], [93]**.

The low cycle fatigue test, which operates under strain control with the load as a dependent variable, is primarily designed to investigate the low cycle fatigue range. This range typically extends from around 10^2 to 10^5 cycles and covers a range of situations where strains can occur in either elastic or plastic regions **[92], [93]**.

The equipment mostly used for high-cycle and low-cycle fatigue tests is shown in **Figure 3.7 [97]** and **Figure 3.8 [98]**.

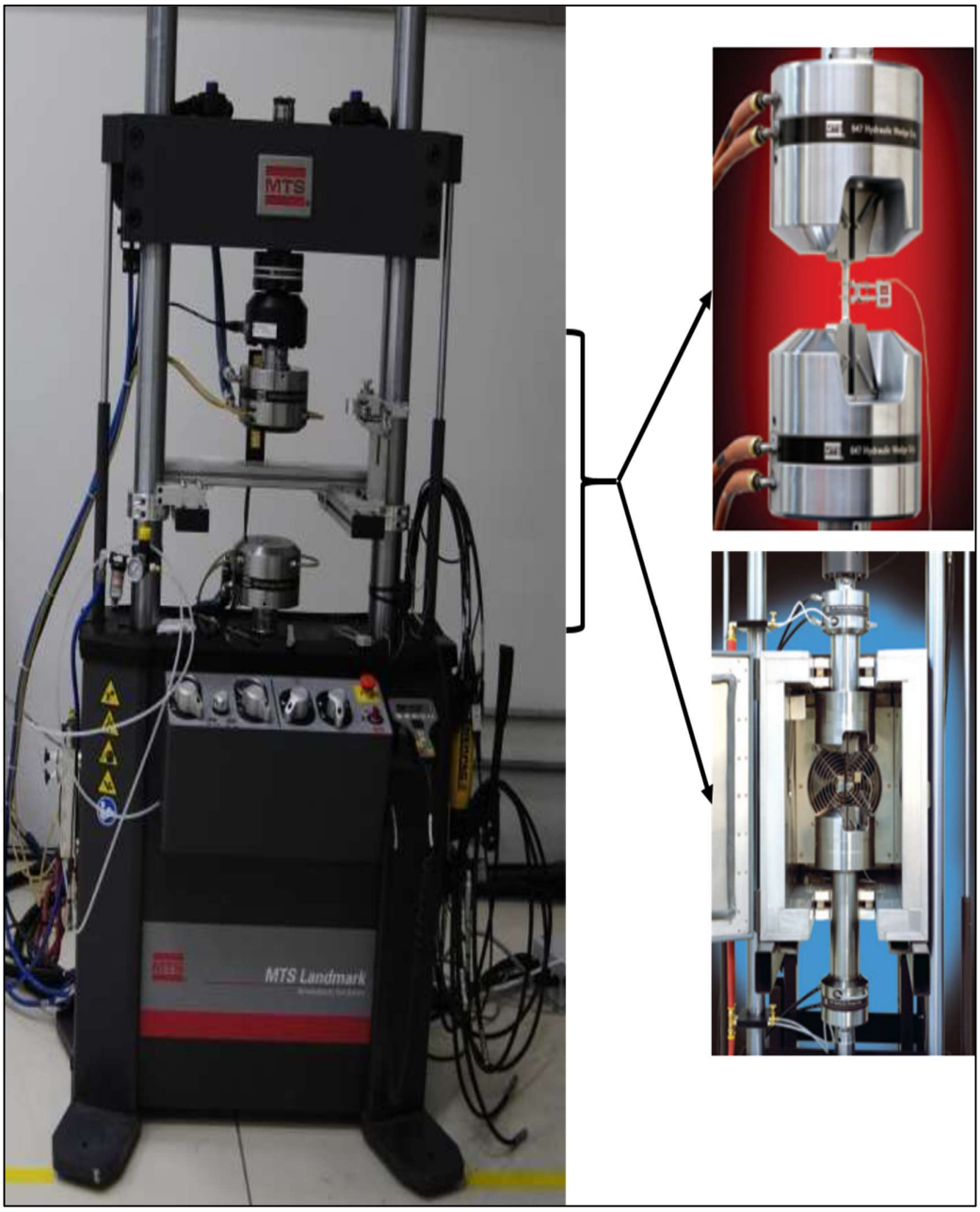

Figure 3.7 : A visual of the MTS Landmark brand test equipment.

MTS landmark test equipment is a servo-hydraulic testing machine. As seen from the photos of the test equipment above, the specimens can be tested under different temperature conditions **[97]**.

Figure 3.8 : A visual of the Zwick/Roell brand test equipment. Adapted from **[98]**.

The ZwickRoell Vibrophore 100 is an advanced testing apparatus that integrates high-frequency pulsators to form an electromagnetically stimulated dynamic testing machine while concurrently maintaining the capabilities of a fully operational static materials testing machine. This versatile equipment allows tests to be conducted under precise control parameters such as force, displacement, and strain. Additionally, by incorporating compatible auxiliary devices, the Vibrophore 100 enables testing to be performed under a wide range of environmental conditions, including torsion and flexure tests **[98]**.

3.3.2. Test Detail and Parameters

The tests were carried out taking into account the following important aspects **[97], [98]**;

- Pull rods are used to test the round specimens, and plain grips are used to test the plain specimens.
- In general, K-type thermocouples are used to control the temperature in high-temperature tests.
- The load axis coincides with the neutral axis of the specimen to avoid unwanted bending mode.
- All equipment has a resolution in accordance with the order of magnitude of the measurement performed. All measuring devices are calibrated prior to performing the tests.
- Appropriate safety devices are installed considering the risk of explosive behavior of the specimen during the rupture test.
- Each 100kN capacity machine is equipped with a load cell of 100kN calibrated according to ASTM E4 and ISO 7500 for servo-hydraulic test equipment. The first point calibrated is 1kN.
- The purpose of high-cycle fatigue testing is to obtain fatigue properties according to ASTM E466.
- The goal of low-cycle fatigue testing, in accordance with ASTM E606, is to determine fatigue properties.

4. RESULTS AND DISCUSSION

In this section, the fatigue test results of Ti-6Al-4V specimens manufactured and post-processed by two different manufacturing methods will be analyzed, compared and discussed in detail. One of the production methods is investment casting, and the other is EB-PBF, an additive manufacturing method. The results of specimens produced with EB-PBF in two different orientations, XY and Z, are emphasized.

4.1. General Information and Test Matrices

When the literature studies are reviewed, although there are extensive studies on L-PBF and EB-PBF methods in terms of fatigue results, there is no comparison between EB-PBF and investment casting methods. For this reason, in order to see the effect of different post processes on fatigue results, the fatigue results of the specimens produced by the EB-PBF method and the investment casting method were compared and analyzed. Fatigue test results and data on specimens produced by both investment casting and EB-PBF methods were obtained from the literature studies.

Fatigue results were analyzed using different test result matrices, as shown in **Table 4.1**.

In the first case, specimens manufactured by the EB-PBF method in XY and Z orientations were examined and compared without machining and without HIP to see the effect of manufacturing orientation on fatigue properties. In the second case, to see the effect of HIP, the results of the specimens produced by the EB-PBF method without machining were examined and compared with and without HIP. In the third case, the machined and unmachined results of the HIP-treated specimens produced by the EB-PBF method were examined and compared to see the effect of machining on fatigue results. In the fourth case, to see the effect of HIP on the fatigue characteristics of the investment cast specimens, the results of the machined specimens were analyzed and compared with and without HIP. In the fifth and final case, the results of machined and HIP-treated specimens produced by the investment casting method and the EB-PBF method were examined and compared to see the effect of the production method on fatigue characteristics.

Table 4.1 : Test comparison matrices based on methods and conditions.

	Production Method	Machining Condition	HIP Condition	Build Orientation
Scenario 1	EB-PBF	Non-Machined	Non-HIP	Vertical
Scenario 2	EB-PBF	Non-Machined	Non-HIP	Horizontal
Scenario 3	EB-PBF	Non-Machined	HIP	Horizontal
Scenario 4	EB-PBF	Machined	HIP	Horizontal
Scenario 5	IC	Machined	Non-HIP	N/A
Scenario 6	IC	Machined	HIP	N/A

4.2. Test Results and Comparisons

In this section, the cases specified in **Table 4.1** are analyzed under sub-headings in a specialized manner.

4.2.1. The Effect of Build Orientation on Fatigue for EB-PBF

In the EB-PBF method, the data of the specimens without HIP and without machining were compared to determine the effect of manufacturing orientation on fatigue characteristics. In other words, scenario 1 and scenario 2, as indicated in **Table 4.1** were compared. In the production orientation, the comparison was made mainly on the results of XY and Z-oriented production specimens. In **Figure 4.1**, the data in blue refers to the XY orientation, and the data in orange refers to the Z orientation.

Comparative results were obtained by utilizing test data from open-source documents in the literature. Test results from the literature are checked for reliability with our own results. Our own results cannot be published due to confidentiality reasons. Both vertical and horizontal fatigue results are retrieved from reference **[99]** to compare the build orientation.

Although fatigue data are limited in the low cycle region ($N<10^4$) for both XY-oriented specimens and Z-oriented specimens, as it can be understood in **Figure 4.1**, the fatigue results of the XY-oriented specimen are better than the Z-oriented specimen results. In

addition to that, as can be understood from the graph in **Figure 4.1**, the endurance limit value of the XY-oriented specimens is approximately 195 to 235 MPa, and the endurance limit value of the Z-oriented specimens is approximately 100 MPa to 150 MPa **[99], [100]**. As a result, the minimum working stress of XY-oriented specimens is higher than that of Z-oriented specimens **[99]**.

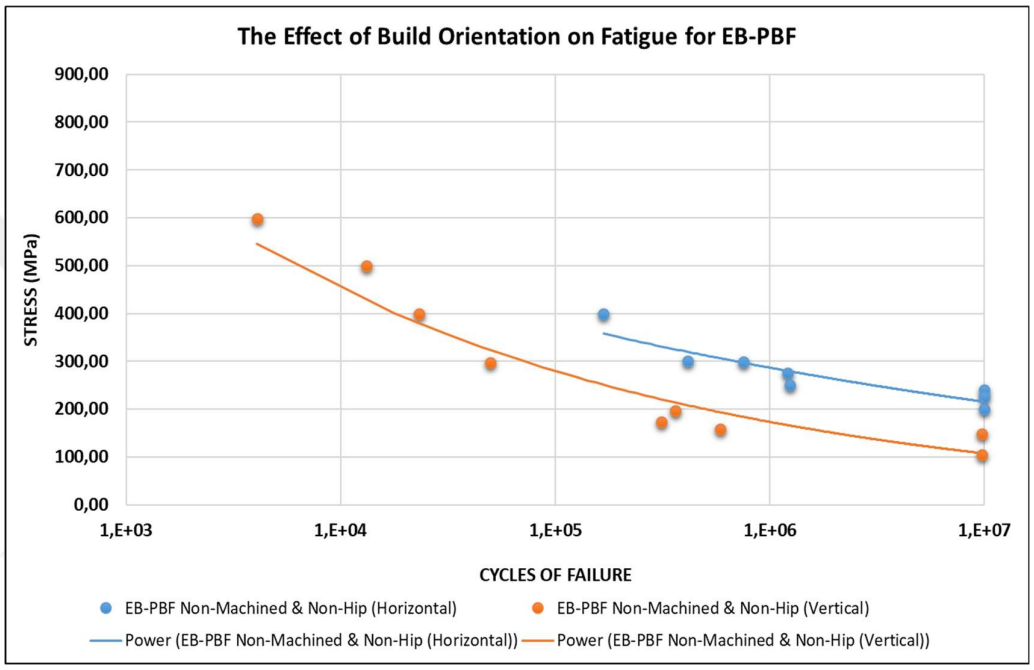

Figure 4.1 : Fatigue characteristic of non-machined & non-hip with Z and XY orientation.

The higher fatigue characteristics of XY-oriented specimens are due to their rough surface. This roughness creates sharp radius notches perpendicular to the feeding direction in Z-oriented specimens, which lead to preferential fracture initiation regions. Compared to the XY-oriented specimens, the fatigue fracture surfaces of Z-oriented specimens are nearly perfect, indicating faster crack initiation and propagation **[99]**.

4.2.2. The Effect of HIP on Fatigue for EB-PBF

In the EB-PBF method, the data of the specimens produced by the EB-PBF method without machining were examined and compared with and without HIP in order to see the effect of HIP. In other words, scenario 2 and scenario 3 as indicated in **Table 4.1**

were compared. In **Figure 4.2**, the data in blue represent the results of EB-PBF samples with HIP, while the data in green represent the results of samples without HIP.

Comparative results were obtained by utilizing test data from open-source documents in the literature. Test results from the literature are checked for reliability with our own results. Our own results cannot be published due to confidentiality reasons. Fatigue results are retrieved from reference **[82], [99]-[103]** to compare the HIP effect for both conditions.

As can be observed in **Figure 4.2**, the deviation rate of the results of the HIP-treated and non-machined specimens is less than the results of the non-HIP-treated and non-machined specimens.

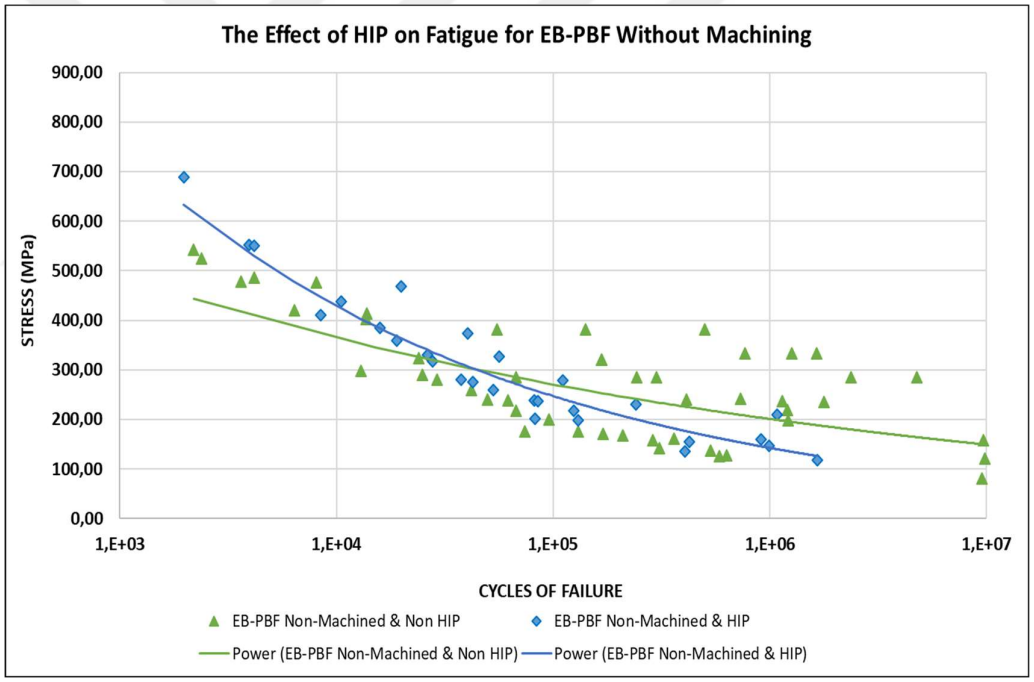

Figure 4.2 : Fatigue characteristic of non-machined with and without HIP.

The combination of microstructural grain coarsening by the HIP process and the rough surface texture from EBM seems to counteract any benefits from reducing porosity in terms of fatigue life. However, although the average fatigue life may appear lower, HIP effectively reduces variability in fatigue data. In the absence of HIP, scatter in fatigue data can occur if defect size surpasses surface roughness, leading to a shift from cracks starting from the surface to internal cracks. HIP ensures pore closure, ensuring fractures initiate solely due to surface effects **[80]**.

4.2.3. The Effect of Machining on Fatigue for EB-PBF

In the EB-PBF method, the data of the specimens that produced by EB-PBF method that HIP treated, with and without machining were analyzed and compared to determine the effect of machining. In other words, scenario 3 and scenario 4 as indicated in **Table 4.1** were compared. In **Figure 4.3**, the data in purple represent the results of HIP-treated and machined EB-PBF samples, while the data in claret represent the results of HIP treated and non-machined samples.

Comparative results were obtained by utilizing test data from open source documents in the literature. Test results from the literature are checked for reliability with our own results. Our own results cannot be published due to confidentiality reasons. Fatigue results are retrieved from references **[100], [102], [104]-[106]** to compare the machining effect for both conditions.

As it can be observed from **Figure 4.3**, the fatigue results of the HIP-treated and machined EB-PBF specimens show better fatigue results than those of the non-machined and HIP-treated specimens. As can be noticed from the graph in **Figure 4.3**, the endurance limit value is in the range of roughly 450-550 MPa for HIP-treated and machined specimens, while the endurance limit value is in the range of roughly 140-160 MPa for HIP-treated and untreated specimens **[100], [107]**. These results show that machining the specimens and thus the elimination of surface roughness has a great contribution to the fatigue characteristics.

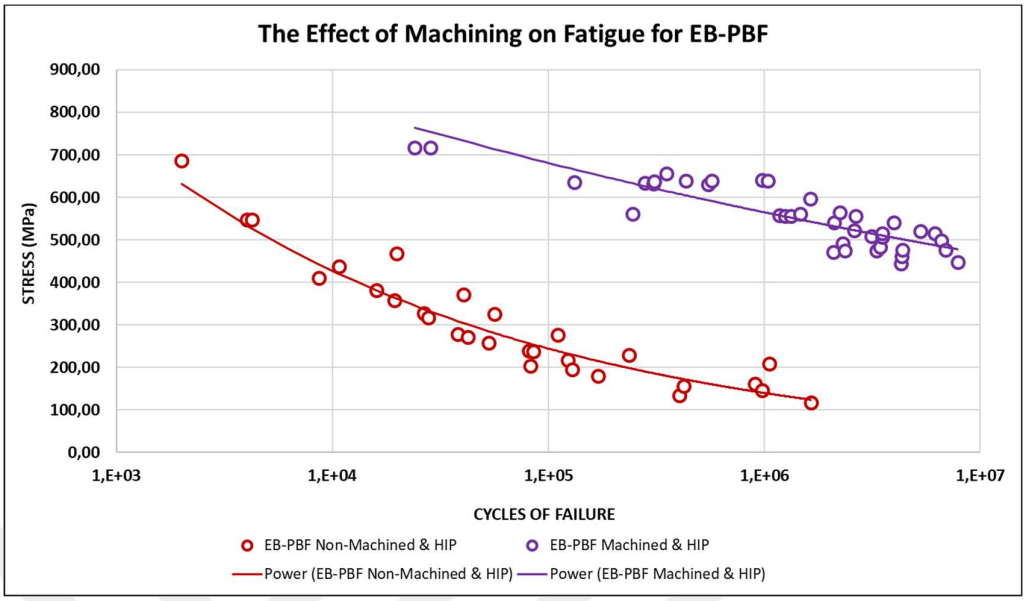

Figure 4.3 : Fatigue characteristic of machined and non-machined HIP specimens.

As surface roughness increases, the stress concentration factor also increases, facilitating the easier formation of fatigue cracks under alternating stress. Consequently, reducing surface roughness is critical to enhance the fatigue resistance of titanium alloy, as it reduces the stress concentration and the probability of fatigue-induced crack initiation **[108]**.

4.2.4. The Effect of HIP on Fatigue for Investment Casting

In the investment casting method, the data of machined specimens produced by the investment casting method with and without HIP were analyzed and compared to determine the effect of HIP. In other words, scenario 5 and scenario 6 as indicated in **Table 4.1** were compared. In **Figure 4.4**, the data in blue represent the results of IC specimens with HIP treated and machined, while the data in green represent the results of specimens without HIP and machined.

Comparative results were obtained by utilizing test data from open-source documents in the literature. Test results from the literature are checked for reliability with our own results. Our own results cannot be published due to confidentiality reasons. Fatigue results are retrieved from reference **[109]-[111]** to compare the HIP effect for the investment casting specimens.

Although fatigue data are limited in the low cycle region ($N<10^4$) for both machined and Non-HIP specimens produced by investment casting and machined and HIP-treated specimens produced by investment casting, as it can be observed in **Figure 4.4**, the fatigue results of the HIP treated and machined specimen show better results than the machined and without HIP specimen results.

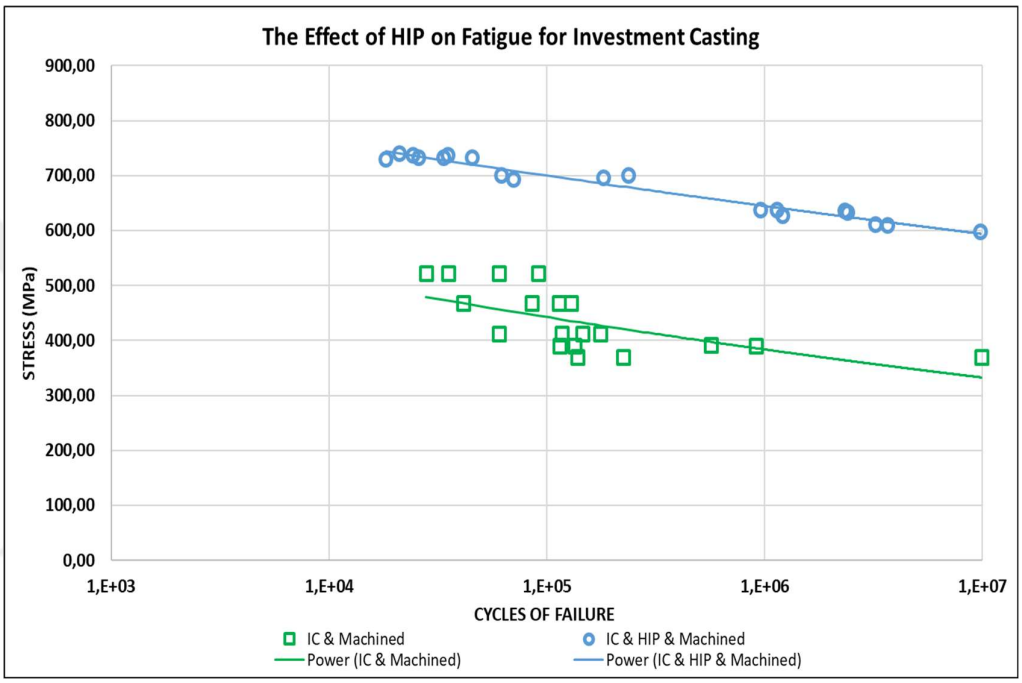

Figure 4.4 : Fatigue characteristic of machined specimens with and without HIP.

It is simple to observe how HIP treatment improves fatigue strength. In titanium alloys, HIP treating removes casting porosity, producing a homogeneous material free of stress concentration points. This porosity removal is particularly important in cast alpha colony formation, where stress concentrations often precipitate basal plane heterogeneous slip and thus accelerate fatigue fracture initiation **[112]**.

4.2.5. The Effect of Manufacturing Method on Fatigue

This section compared and evaluated the machined and HIP treated specimens generated by the EB-PBF method and the investment casting method to determine how the manufacturing method affected the fatigue characteristics. In other words, scenario 4 and scenario 6 as indicated in **Table 4.1** were compared. In **Figure 4.5**, the data in blue represent the results of IC specimens with HIP-treated and machined, while the

data in green represent the results of EB-PBF specimens with HIP-treated and machined.

Comparative results were obtained by utilizing test data from open-source documents in the literature. Test results from the literature are checked for reliability with our own results. Our own results cannot be published due to confidentiality reasons. Fatigue results are retrieved from references **[100], [102], [104]-[106], [109]-[111]** to compare both manufacturing methods.

As it can also be seen from **Figure 4.5**, the fatigue results of the HIP-treated and machined IC specimens show better fatigue results than those of the machined and HIP-treated EB-PBF specimens. In addition to that, as can be observed from the graph in **Figure 4.5**, the endurance limit value is in the range of roughly 600 MPa for HIP-treated and machined IC specimens, while the endurance limit value is in the range of roughly 450-530 MPa for HIP treated and machined specimens **[112], [113**]. As a result, the minimum working stress of IC specimens is higher than that of EB-PBF specimens.

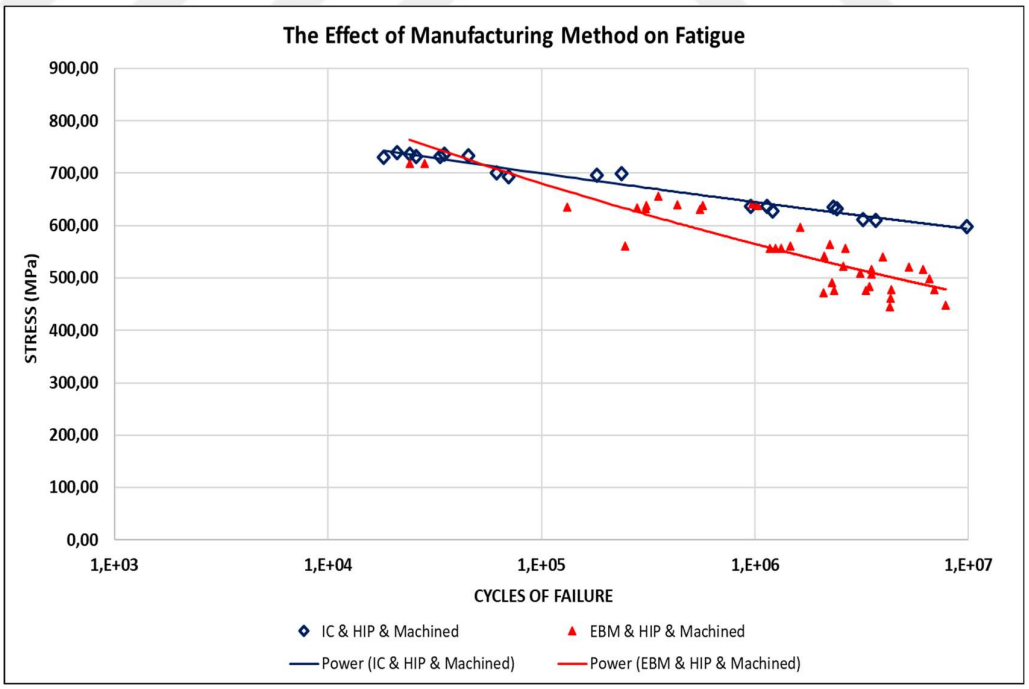

Figure 4.5 : Fatigue characteristic of EB-PBF and IC specimens.

In investment casting, the damage mechanisms are largely due to microstructural reasons. Therefore, the investment casting method's specimens exhibit better fatigue performance than the EB-PBF method's specimens **[114]**.

4.2.6. Fatigue Test Results of Specimens Produced by AM

As mentioned in the previous sections, fatigue test results could not be shared for both cast and additive manufacturing specimens due to project confidentiality. Fatigue tests have been performed on Z-oriented additive manufacturing specimens produced outside the scope of the project, and the results are shared below. The specimens have been heat-treated and machined specimens and have not been subjected to HIP operation. The fatigue tests were conducted at room temperature, with an R=0.1 fatigue stress ratio and maximum stress values of 350-400 MPa. The test results and related parameters are given in **Table 4.2.**

Table 4.2 : Test results and test parameters of the AM specimens

Maximum Stress (MPa)	Minimum Stress (Mpa)	Ambient Temperature (°C)	Life Cycles	Frequency (Hz)	Failure Location
400	40	26.1	4576	60	Gage Section
350	35	26.2	22240	60	Gage Section
400	40	25.1	1705392	60	Gage Section
350	35	25.2	59568	60	Gage Section

The test findings show that there are deviations in the specimens without HIP's fatigue results. This also confirms the results in **Figure 4.2**. HIP leads to porosity closure, allowing fractures to initiate only due to surface effects. In addition to that, HIP operation also effectively reduces variability and deviations in fatigue data.

5. CONCLUSION

In this chapter, the results of fatigue tests of Ti-6Al-4V specimens manufactured and post-processed by two types of production methods in the literature are evaluated. Suggestions for further studies are also given.

5.1. General Conclusions

In this thesis, based on the studies in the literature, the results of the effect of production orientation, HIP process, and machining operation on the specimens produced by the EB-PBF, the effect of the HIP process on the specimens produced by investment casting method and finally the results of the comparison of the two production methods in terms of fatigue characteristics are given below:

Comparative results were obtained by utilizing test data from open-source documents in the literature. The test results from the literature were checked for accuracy with our own results. Our own results could not be published due to confidentiality reasons.

- Examination and comparisons were made on the fatigue results of both vertically oriented and horizontally oriented specimens manufactured by the EB-PBF method, and the results of the horizontally oriented specimens showed better results than the vertically oriented ones. The roughness caused by the production orientation creates notches with sharp radii perpendicular to the feed direction in vertically oriented specimens, leading to fracture initiation and propagation.
- Fatigue characteristic examinations and comparisons were made on the specimens with and without HIP treatment of the specimens that were not machined by the EB-PBF method. Although there are not very different values in the examination results, the results of the HIP-treated specimens have less variation. In the non-HIP treated specimens, it was observed that there was dispersion in the data. These results show that the beginning of fatigue damage starts from the surface of the specimens and progresses inside. This is the reason why the HIP process is not so effective on the fatigue life of the material.

- Fatigue characteristic examinations and comparisons were made between the EB-PBF method and HIP-treated specimens on machined and non-machined specimens. The findings demonstrated that the surface roughness of the specimens directly increases the stress concentration factor and causes fatigue cracks to form under stress. The machining operation improved the surface roughness and prevented fatigue crack initiation. HIP-treated and machined specimens showed superior fatigue results compared to HIP-treated and non-machined specimens.
- Fatigue characteristic investigations and comparisons were made between HIP-treated and untreated specimens produced by the investment casting method on machined specimens. The HIP process eliminates the porosity of the investment casting and the indications from the production method, thus avoiding stress concentration areas. As a result, a beneficial effect on fatigue characteristics was observed.
- Fatigue characteristic investigations and comparisons were made on machined and HIP-treated specimens produced by investment casting and the EB-PBF method. Due to the differences in microstructure and layered structure of the EB-PBF specimens, the fatigue results of the specimens produced by the investment casting method are better than EB-PBF.

5.2. Recommendations for Future Studies

Regarding the area of advanced manufacturing, EB-PBF is rapidly emerging as a game-changing force with the power to produce complex metallic parts suitable for real-world applications. Research in this field is rapidly expanding and a large number of topics are being explored. The following areas can be explored as future studies:

- Investigating how variations in process parameters, including energy input, scanning strategy, and powder characteristics, affect fatigue properties.
- Understanding the correlation between microstructural features (e.g., grain size, phase distribution, defects) and fatigue behavior to develop strategies for controlling microstructure to enhance fatigue resistance.

- Exploring the effects of surface finishing methods (e.g., machining, shot peening, polishing) on fatigue performance and identifying the most effective techniques for improving fatigue resistance.
- Assessing the impact of post-processing treatments including heat treatment and surface quality improvement on fatigue properties to mitigate potential fatigue-sensitive defects and enhance material properties.

REFERENCES

[1] Donachie, M. J., (2000). Titanium: a technical guide. ASM international.

[2] Leyens, C., & Peters, M., (2003). Titanium and Titanium Alloys: Fundamentals and Applications. John Wiley & Sons.

[3] Williams, J. C., & Boyer, R. R., (2020). Opportunities and issues in the application of titanium alloys for aerospace components. Metals, 10(6), 705.

[4] Kobryn, P. A., (2008). Casting of Titanium alloys. National Technical Information Service.

[5] Blakey-Milner, B., Gradl, P. R., Snedden, G., Brooks, M. J., Pitot, J., López, E., Leary, M., Berto, F., & Du Plessis, A., (2021). Metal additive manufacturing in aerospace: A review. Materials & Design, 209, 110008. https://doi.org/10.1016/j.matdes.2021.110008.

[6] Najmon, J. C., Raeisi, S., & Tovar, A., (2019). Review of additive manufacturing technologies and applications in the aerospace industry. Additive manufacturing for the aerospace industry, 7-31.

[7] Doğu, M. N., (2019). Production of Ti-6Al-4V alloy by 3D electron beam melting technique and development of its post treatments (Master's thesis, Middle East Technical University).

[8] Allen, P., (1996). Titanium alloy development. Advanced Materials & Processes, 150(4), 35.

[9] Welsch, G., Boyer, R., & Collings, E. W. (Eds.)., (1993). Materials properties handbook: titanium alloys. ASM international.

[10] Henriques, V. A., (2009). Titanium production for aerospace applications. Journal of aerospace technology and management, 1, 7-17.

[11] Walter, J. L., Jackson, M. R., & Sims, C. T., (1988). Titanium and its alloys: principles of alloying titanium. ASM Int., Materials Park, OH, 1.

[12] Boyer, R. R., & Briggs, R. D., (2005). The use of β titanium alloys in the aerospace industry. Journal of Materials Engineering and Performance, 14, 681-685.

[13] Hanson, B., (1995). The selection and use of titanium: a design guide. Institute of Materials.

[14] Joseph, S. S., & Froes, F. H., (1988). Titanium metallurgy and applications. Light Metal Age, Vol46, No. 11, pp. 5-12.

[15] Lütjering, G., & Williams, J. C., (2007). Titanium matrix composites (pp. 367-382). Springer Berlin Heidelberg.

[16] Lütjering, G. E. R. D., (1998). Influence of processing on microstructure and mechanical properties of (α+ β) titanium alloys. Materials Science and Engineering: A, 243(1-2), 32-45.

[17] Gil, F. J., Ginebra, M. P., Manero, J. M., & Planell, J. A., (2001). Formation of α-Widmanstätten structure: effects of grain size and cooling rate on the Widmanstätten morphologies and on the mechanical properties in Ti6Al4V alloy. Journal of Alloys and Compounds, 329(1-2), 142-152.

[18] Horton, R. A., (1988). "Investment Casting," (Ninth Edition, Vol. 15). Metals Handbook (pp. 253–269).

[19] Pattnaik, S., Karunakar, D. B., & Jha, P. K., (2012). Developments in investment casting process—A review. Journal of Materials Processing Technology, 212(11), 2332-2348.

[20] Investment Casting Process Steps and Flow Chart | American Casting Company. (2019, July 9). American Casting Company. https://americancastingco.com/investment-casting-process/

[21] Laszeray. (2023). Investment casting: Steps in the investment casting process. *Laszeray Technology*. https://laszeray.com/investment-casting-steps-in-the-investment-casting-process/

[22] David. (2023). What is Investment Casting? *Reliance Foundry Co. Ltd*. https://www.reliance-foundry.com/blog/investment-casting.

[23] Eyion, D., J. R. Newman, and J. K. Thome, "*Titanium and Titanium Alloy Castings,*" Metals Handbook, Tenth Edition, v. 2, pp. 637-644, 1990.

[24] Lei, C. S. C., Frazier, W. E., & Lee, E. W., (1997). The effect of hot isostatic pressing on cast aluminum. JOM, 49(11), 38–39.

[25] Lutjering G., Gysler A. *Titanium science and technology*, Vol. 4, 1985, p. 2068.

[26] Zhang, Y., Jarosinski, W., Jung, Y. G., & Zhang, J., (2018). Additive manufacturing processes and equipment. In Additive manufacturing (pp. 39-51). Butterworth-Heinemann.

[27] Sames, W. J., List, F. A., Pannala, S., Dehoff, R. R., & Babu, S. S., (2016). The metallurgy and processing science of metal additive manufacturing. International materials reviews, 61(5), 315-360.

[28] Standard Terminology for Additive Manufacturing Technologies. (2012). *ASTM International (2012).* https://doi.org/10.1520/f2792-12a.

[29] Jacops P. F., (1995). Stereolithography and other PP and M technologies: from rapid prototyping to rapid tooling. New York: SME.

[30] 3D Hubs. (2018, June 18). 3 Additive Manufacturing technologies to watch out for in 2017. *Medium*. https://medium.com/extreme-engineering/3-additive-manufacturing-technologies-to-watch-out-for-in-2017-7226d310ca56

[31] Hopkinson, N., Hague, R. J. M., & Dickens, P., (2006b). Rapid manufacturing: An Industrial Revolution for the Digital Age. John Wiley & Sons, 5-18.

[32] Burns, M., (1993). Automated fabrication: improving productivity in manufacturing. Prentice-Hall, Inc..

[33] Frazier, W. E., (2014). Metal additive manufacturing: a review. Journal of Materials Engineering and performance, 23, 1917-1928.

[34] Ngo, T. D., Kashani, A., Imbalzano, G., Nguyen, K. T., & Hui, D., (2018). Additive manufacturing (3D printing): A review of materials, methods, applications and challenges. Composites Part B: Engineering, 143, 172-196.

[35] Kumar, L. J., & Krishnadas Nair, C. G., (2017). Current trends of additive manufacturing in the aerospace industry. Advances in 3D printing & additive manufacturing technologies, 39-54.

[36] Pettersson, A. B. V., Salmi, M., Vallittu, P., Serlo, W., Tuomi, J., & Mäkitie, A. A., (2020). Main clinical use of additive manufacturing (three-dimensional printing) in Finland restricted to the head and neck area in 2016–2017. Scandinavian journal of surgery, 109(2), 166-173.

[37] Zadpoor, A. A., & Malda, J., (2017). Additive manufacturing of biomaterials, tissues, and organs. Annals of biomedical engineering, 45, 1-11.

[38] Zadpoor, A. A., (2015). Bone tissue regeneration: the role of scaffold geometry. Biomaterials science, 3(2), 231-245.

[39] Massachusetts Institute of Technology. (n.d.). With 3-D printing, the shoe really fits | MIT Sloan Management Review. MIT Sloan Management Review. https://sloanreview.mit.edu/article/with-3-d-printing-the-shoe-really-fits/

[40] Meier, M., Tan, K. H., Lim, M. K., & Chung, L., (2018). Unlocking innovation in the sport industry through additive manufacturing. Business Process Management Journal, 25(3), 456-475.

[41] Peterson, A. (n.d.). Utilization of recycled filament for 3D printing for consumer goods. ScholarWorks@UARK. https://scholarworks.uark.edu/ampduht/13

[42] Janssens, A., & Lavanga, M., (2018). An Expensive, Confusing, and Ineffective Suit of Armor: Investigating Risks of Design Piracy and Perceptions of the Design Rights Available to Emerging Fashion Designers in the Digital Age. Fashion Theory, 24, 229 - 260.

[43] Sun, J., Peng, Z., Zhou, W., Fuh, J. Y., Hong, G. S., & Chiu, A., (2015). A review on 3D printing for customized food fabrication. Procedia Manufacturing, 1, 308-319.

[44] Severini, C., Derossi, A., & Azzollini, D., (2016). Variables affecting the printability of foods: Preliminary tests on cereal-based products. Innovative food science & emerging technologies, 38, 281-291.

[45] Hao, L., Mellor, S., Seaman, O., Henderson, J., Sewell, N., & Sloan, M., (2010). Material characterisation and process development for chocolate additive layer manufacturing. Virtual and Physical Prototyping, 5(2), 57-64.

[46] Pegna, J., (1997). Exploratory investigation of solid freeform construction. Automation in construction, 5(5), 427-437.

[47] Wu, P., Wang, J., & Wang, X., (2016). A critical review of the use of 3-D printing in the construction industry. Automation in Construction, 68, 21-31.

[48] Coykendall, J., Cotteleer, M., Holdowsky, J., & Mahto, M., (2014). 3D opportunity in aerospace and defense: Additive manufacturing takes flight. A Deloitte series on additive manufacturing, 1.

[49] Chua, C. K., Leong, K. F., & Lim, C. S., (2003). Rapid prototyping: Principles and Applications. World Scientific, 25–33.

[50] Murr, L. E., Gaytan, S. M., Ramirez, D. A., Martinez, E., Hernandez, J., Amato, K. N., Shindo, P. W., Medina, F., & Wicker, R. B., (2012). Metal fabrication by additive manufacturing using laser and electron beam melting technologies. Journal of Materials Science & Technology, 28(1), 1–14. https://doi.org/10.1016/s1005-0302(12)60016-4.

[51] Bai, Y., & Williams, C. B., (2015). An exploration of binder jetting of copper. Rapid Prototyping Journal, 21(2), 177-185.

[52] Sova, A., Grigoriev, S., Okunkova, A., & Smurov, I., (2013). Potential of cold gas dynamic spray as additive manufacturing technology. The International Journal of Advanced Manufacturing Technology, 69, 2269-2278.

[53] Zenou, M., & Grainger, L., (2018). Additive manufacturing of metallic materials. In Additive manufacturing (pp. 53-103). Butterworth-Heinemann.

[54] Thompson, S.M., Bian, L., Shamsaei, N., & Yadollahi, A., (2015). An overview of Direct Laser Deposition for additive manufacturing; Part I: Transport phenomena, modeling and diagnostics. Additive manufacturing, 8, 36-62.

[55] Gibson, I., Rosen, D. W., Stucker, B., Khorasani, M., Rosen, D., Stucker, B., & Khorasani, M., (2021). Additive manufacturing technologies (Vol. 17, pp. 160-186). Cham, Switzerland: Springer.

[56] Parthasarathy, J., Starly, B., Raman, S., & Christensen, A., (2010). Mechanical evaluation of porous titanium (Ti6Al4V) structures with electron beam melting (EBM). Journal of the mechanical behavior of biomedical materials, 3(3), 249-259.

[57] The unrealised potential of Electron Beam Powder Bed Fusion. (2023, June 13). Metal AM Magazine. https://www.metal-am.com/articles/unrealised-potential-the-story-and-status-of-electron-beam-powder-bed-fusion-3d-printing/

[58] Yadroitsev, I., Yadroitsava, I., Du Plessis, A., & MacDonald, E. (Eds.)., (2021). Fundamentals of laser powder bed fusion of metals. Elsevier.

[59] Yap, C. Y., Chua, C. K., Dong, Z. L., Liu, Z. H., Zhang, D. Q., Loh, L. E., & Sing, S. L., (2015). Review of selective laser melting: Materials and applications. Applied physics reviews, 2(4).

[60] Enteknograte. (2023). Finite element simulation of powder bed fusion processes - enteknograte. Enteknograte. https://enteknograte.com/additive-manufacturing-process-simulation/powder-bed-fusion-processes-finite-element-simulation/.

[61] Bhavar, V., Kattire, P., Patil, V., Khot, S., Gujar, K., & Singh, R., (2017). A review on powder bed fusion technology of metal additive manufacturing. Additive manufacturing handbook, 251-253.

[62] Gu, D. D., Meiners, W., Wissenbach, K., & Poprawe, R., (2012). Laser additive manufacturing of metallic components: materials, processes and mechanisms. International materials reviews, 57(3), 133-164.

[63] Kruth, J. P., Mercelis, P., Van Vaerenbergh, J., Froyen, L., & Rombouts, M., (2005). Binding mechanisms in selective laser sintering and selective laser melting. Rapid prototyping journal, 11(1), 26-36.

[64] Uriondo, A., Esperon-Miguez, M., & Perinpanayagam, S., (2015). The present and future of additive manufacturing in the aerospace sector: A review of important aspects. Proceedings of the Institution of Mechanical Engineers, Part G: Journal of Aerospace Engineering, 229(11), 2132-2147.

[65] Heralić, A., Christiansson, A. K., & Lennartson, B., (2012). Height control of laser metal-wire deposition based on iterative learning control and 3D scanning. Optics and lasers in engineering, 50(9), 1230-1241.

[66] Liu, R., Wang, Z., Sparks, T., Liou, F., & Newkirk, J., (2017). Aerospace applications of laser additive manufacturing. In Laser additive manufacturing (pp. 351-371). Woodhead Publishing.

[67] Mudge, R. P., & Wald, N. R., (2007). Laser engineered net shaping advances additive manufacturing and repair. Welding Journal-New York-, 86(1), 44.

[68] Portolés, L., Jordá, O., Jordá, L., Uriondo, A., Esperon-Miguez, M., & Perinpanayagam, S., (2016). A qualification procedure to manufacture and repair aerospace parts with electron beam melting. Journal of Manufacturing Systems, 41, 65-75.

[69] Wang, Z., Liu, R., Sparks, T., Liu, H., & Liou, F., (2015). Stereo vision based hybrid manufacturing process for precision metal parts. Precision Engineering, 42, 1-5.

[70] Oyelola, O., Crawforth, P., M'Saoubi, R., & Clare, A. T., (2018). On the machinability of directed energy deposited Ti6Al4V. Additive Manufacturing, 19, 39-50.

[71] Lim, J. S., Oh, W. J., Lee, C. M., & Kim, D. H., (2021). Selection of effective manufacturing conditions for directed energy deposition process using machine learning methods. Scientific reports, 11(1), 24169.

[72] Nematollahi, M., Jahadakbar, A., Mahtabi, M. J., & Elahinia, M., (2019). Additive manufacturing (AM). In Metals for biomedical devices (pp. 331-353). Woodhead Publishing.

[73] Domack, M. S., Taminger, K. M., & Begley, M., (2006, July). Metallurgical mechanisms controlling mechanical properties of aluminium alloy 2219 produced by electron beam freeform fabrication. In Materials science forum (Vol. 519, pp. 1291-1296). Trans Tech Publications Ltd.

[74] Cruson, D. (n.d.-b). What is Directed Energy Deposition (DED) 3D Printing? | Sciaky. https://www.sciaky.com/additive-manufacturing/what-is-ded-3d-printing.

[75] Boyer, R. R., (1996). An overview on the use of titanium in the aerospace industry. Materials Science and Engineering: A, 213(1-2), 103-114.

[76] Cui, C., Hu, B., Zhao, L., & Liu, S., (2011). Titanium alloy production technology, market prospects and industry development. Materials & Design, 32(3), 1684-1691.

[77] Liu, S., & Shin, Y. C., (2019). Additive manufacturing of Ti6Al4V alloy: A review. Materials & Design, 164, 107552.

[78] Gong, H., Rafi, K., Gu, H., Ram, G. J., Starr, T., & Stucker, B., (2015). Influence of defects on mechanical properties of Ti–6Al–4 V components produced by selective laser melting and electron beam melting. Materials & Design, 86, 545-554.

[79] Rafi, H. K., Karthik, N. V., Gong, H., Starr, T. L., & Stucker, B. E., (2013). Microstructures and mechanical properties of Ti6Al4V parts fabricated by selective laser melting and electron beam melting. Journal of materials engineering and performance, 22, 3872-3883.

[80] Chern, A. H., Nandwana, P., Yuan, T., Kirka, M. M., Dehoff, R. R., Liaw, P. K., & Duty, C. E., (2019). A review on the fatigue behavior of Ti-6Al-4V fabricated by electron beam melting additive manufacturing. International journal of fatigue, 119, 173-184.

[81] Wycisk, E., Solbach, A., Siddique, S., Herzog, D., Walther, F., & Emmelmann, C., (2014). Effects of defects in laser additive manufactured Ti-6Al-4V on fatigue properties. Physics Procedia, 56, 371-378.

[82] Edwards, P., O'conner, A., & Ramulu, M., (2013). Electron beam additive manufacturing of titanium components: properties and performance. Journal of Manufacturing Science and Engineering, 135(6), 061016.

[83] Li, P., Warner, D. H., Fatemi, A., & Phan, N., (2016). Critical assessment of the fatigue performance of additively manufactured Ti–6Al–4V and perspective for future research. International Journal of Fatigue, 85, 130-143.

[84] Eylon, D., (1979). Fatigue crack initiation in hot isostatically pressed Ti-6Al-4V castings. Journal of Materials Science, 14, 1914-1922.

[85] Pilchak, A. L., & Williams, J. C., (2009). Effect of yttrium on the fatigue behavior of investment-cast and wrought Ti-6Al-4V. Metallurgical and Materials Transactions A, 40, 2603-2615.

[86] Yoder, G. R., Cooley, L. A., & Crooker, T. W., (1978). Fatigue crack propagation resistance of beta-annealed Ti-6AI-4V alloys of differing interstitial oxygen contents. Metallurgical Transactions A, 9, 1413-1420.

[87] Hornberger, H., Randow, C., & Fleck, C., (2015). Fatigue and surface structure of titanium after oxygen diffusion hardening. Materials Science and Engineering: A, 630, 51-57.

[88] Inagaki, I., Takechi, T., Shirai, Y., & Ariyasu, N., (2014). Application and features of titanium for the aerospace industry. Nippon steel & sumitomo metal technical report, 106(106), 22-27.

[89] Yanko, T., & Dmytrenko, O., (2021). Prospects for the implementation of new materials and technologies in the aerospace industry. Transactions on Aerospace Research, 2021(4), 1-10.

[90] Zhang, Y., (2024, January 15). CNC machining of Titanium & Alloys. CNC Machining Service, Rapid Prototyping. https://proleantech.com/cnc-machining-of-titanium-alloys/#Applications

[91] Compare all products from Arcam - 3Dnatives. (n.d.). Comparator. https://www.3dnatives.com/3D-compare/en/manufacturer/arcam-en/

[92] Yılmaz, F., (2022). Mechanical characterization of additively manufactured Ti-6Al-4V aircraft structural components produced by electron beam melting.

[93] Keough, C. B., (2020). Fatigue Performance of Additively Manufactured Ti-6Al-4V: Influence of Build Orientation and Secondary Processing. North Carolina State University.

[94] Temel Yiğitbaşı, S., (2018). Mechanical properties of Ti6Al4V parts produced by electron beam melting and topology optimization in different building directions (Master's thesis, Middle East Technical University).

[95] Eylon, D., Froes, F. H., & Levin, L., (1985). Effect of hot isostatic pressing and heat treatment on fatigue properties of Ti-6 Al-4 V castings. Titanium: Science and technology, 179-186.

[96] Eylon, D., Froes, F. H., & Gardiner, R. W., (1983). Developments in titanium alloy casting technology. JOM, 35(2), 35-47.

[97] MTS Landmark® Testing Solutions. (n.d.-b). MTS Systems. https://www.mts.com/-/media/materials/pdfs/brochures/mts-landmark-test-system-brochure.pdf?as=1

[98] Product Information ZwickRoell Vibrophore 100. (n.d.). ZwickRoell. https://www.zwickroell.com/fileadmin/content/Files/SharePoint/user_upload/PI_EN/13_890_Vibrophore_100_PI_EN.pdf

[99] Khalid Rafi, H., Karthik, N. V., Starr, T. L., & Stucker, B. E., (2012). Mechanical property evaluation of Ti-6Al-4V parts made using Electron Beam Melting.

[100] Greitemeier, D., Palm, F., Syassen, F., & Melz, T., (2017). Effect of surface roughness on fatigue performance of additive manufactured Ti–6Al–4V

[101] Greitemeier, D., Palm, F., Syassen, F., & Melz, T., (2017). Fatigue performance of additive manufactured TiAl6V4 using electron and laser beam melting. International Journal of Fatigue, 94, 211-217.

[102] Witkin, D. B., Albright, T. V., & Patel, D. N., (2016). Empirical approach to understanding the fatigue behavior of metals made using additive manufacturing. Metallurgical and Materials Transactions A, 47, 3823-3836.

[103] Peter, W. H., Nandwana, P., Kirka, M. M., Dehoff, R. R., Sames, W., Erdman III, D. L., ... & Howard, R., (2015). Understanding the role of hot isostatic pressing parameters on the microstructural evolution of Ti-6Al-4V and Inconel 718 fabricated by electron beam melting (No. ORNL/TM-2015/77). Oak Ridge National Lab.(ORNL), Oak Ridge, TN (United States).

[104] Ackelid, U., & Svensson, M., (2009, October). Additive manufacturing of dense metal parts by electron beam melting. In Proceedings of the Materials Science and Technology Conference, Pittsburgh, PA, USA (Vol. 2529, p. 9).

[105] Brandl, E., Leyens, C., & Palm, F., (2011, December). Mechanical properties of additive manufactured Ti-6Al-4V using wire and powder based processes. In IOP conference series: materials science and engineering (Vol. 26, No. 1, p. 012004). IOP Publishing.

[106] Mohammadhosseini, A., Fraser, D., Masood, S. H., & Jahedi, M., (2013). Microstructure and mechanical properties of Ti–6Al–4V manufactured by electron beam melting process. Materials Research Innovations, 17(sup2), s106-s112.

[107] Hrabe, N., Gnäupel-Herold, T., & Quinn, T., (2017). Fatigue properties of a titanium alloy (Ti–6Al–4V) fabricated via electron beam melting (EBM): Effects of internal defects and residual stress. International Journal of Fatigue, 94, 202-210.

[108] Du, D. X., Liu, D. X., Sun, Y. F., Tang, J. G., & Zhang, X. H., (2012). The effects of machined workpiece surface integrity on the fatigue life of TC21 titanium alloy. Advanced Materials Research, 503, 382-389.

[109] Oh, J., Lee, J. G., Kim, N. J., Lee, S., & Lee, E. W., (2004). Effects of thickness on fatigue properties of investment cast Ti-6Al-4V alloy plates. Journal of materials science, 39, 587-591.

[110] Lin, C. W., Ju, C. P., & Lin, J. H. C., (2005). A comparison of the fatigue behavior of cast Ti–7.5 Mo with cp titanium, Ti–6Al–4V and Ti–13Nb–13Zr alloys. Biomaterials, 26(16), 2899-2907.

[111] Léopold, G., Nadot, Y., Billaudeau, T., & Mendez, J., (2015). Influence of artificial and casting defects on fatigue strength of moulded components in Ti-6Al-4V alloy. Fatigue & Fracture of Engineering Materials & Structures, 38(9), 1026-1041.

[112] Cao, F., Zhang, T., Ryder, M. A., & Lados, D. A., (2018). A review of the fatigue properties of additively manufactured Ti-6Al-4V. Jom, 70, 349-357.

[113] Adachi, S., Wagner, L., & Lütjering, G., (1985). Influence of microstructure and mean stress on fatigue strength of Ti-Al-4 V. Titanium: Science and technology, 2139-2146.

[114] Nastac, L., Gungor, M. N., Üçok, I., Klug, K. L., & Tack, W. T., (2006). Advances in investment casting of Ti–6Al–4V alloy: a review. International Journal of Cast Metals Research, 19(2), 73–93. https://doi.org/10.1179/136404605225023225.

BIOGRAPHY

The author, Kerem SELVİ, started his career as a Technical Consultant in the industrial automation sector. He is currently working as an Advanced Lead Engineer in the aviation industry.